NASA Technical Memorandum 78657

RECTANGULAR CAPTURE AREA TO CIRCULAR COMBUSTOR SCRAMJET ENGINE

S. Zane Pinckney

MARCH 1978

National Aeronautics and Space Administration

Langley Research Center
Hampton, Virginia 23665

RECTANGULAR CAPTURE AREA TO CIRCULAR COMBUSTOR SCRAMJET ENGINE

by

S. Zane Pinckney
Langley Research Center

SUMMARY

A concept for a new scramjet engine design is presented. This engine has a projected capture area which is rectangular in shape with a center body which has a 20° included angle cone followed by a constant diameter cylinder. The inlet leading edges are, in general, swept from top to cowl with notches in all leading edges. The method of design of the inlet inner surface is that of streamline tracing. The inlet transforms the rectangular capture stream tube into a cross section which is almost circular shape at the strut leading edges. The high pressure and temperature regions of the combustor are almost circular in shape and, thus, the benefits of hoop stresses in relation to structural weights can be utilized to reduce combustor and engine weights. The fuel struts, which are located in a radial array at the throat of the inlet, pass from the center body to the inlet inner surface and are swept 54° relative to the center body. Strut length to maximum average thickness ratios are between 5.6 and 6.6, which are felt to be structurally reasonable. Strut leading edges lie on a surface which is swept from engine top to the cowl to facilitate flow spillage out through the bottom of the inlet during inlet start and normal operation. For $M_\infty = 6.0$ and $M_1 = 5.58$, the ratio of combustor wetted area to cowl area of the new engine concept is 5.54 as compared to 7.6 for the all rectangular module; for $M_\infty = 4.0$ and $M_1 = 3.54$, the ratio of combustor wetted area to cowl area is 10.07 as compared to 12.86. This decrease in combustor wetted area is offset somewhat by an increase in inlet wetted area. Proof of the correct inlet and combustor configuration can only be accomplished through experimental testing.

INTRODUCTION

To minimize vehicle requirements such as gross weight and fuel load for performing a mission, the scramjet engine should have at least three desirable characteristics (ref. 1). First, the engine performance should be good over the desired Mach number range; second, the engine should be able to cool itself regeneratively; and third, the engine should be light in weight. Also, for a scramjet engine other desirable engine characteristics are that the engine be fixed geometry, self starting, and have inlet entrance and nozzle exit shapes which permit the engine to be integrated into a typical aircraft configuration

(ref. 2). Evaluation of engine performance should be from the viewpoint of installed performance as indicated in the investigations of references 1 through 5.

A candidate for the desired engine is the Langley scramjet engine module discussed in references 2 through 8. This engine module is fixed geometry with a cross-sectional shape that is rectangular and side walls that are swept planar surfaces. The inlet is self starting (refs. 6 and 7) and estimates of installed performance (ref. 4 for M_∞ = 5 to 7) and engine cooling (refs. 2, 3, and 5) indicate the Langley scramjet modular engine will satisfy both the performance and regenerative cooling requirements for long range hypersonic flight. In order to satisfy regenerative cooling requirements, fuel injection struts are used to shorten the combustor and reduce combustor wetted areas (ref. 3); when possible supersonic combustion is used instead of subsonic combustion and inlet contraction ratio is below 10 (refs. 2, 7, and 8). Two basic characteristics of the Langley scramjet engine module design result in its satisfying the engine aircraft integration requirements. First is the rectangular shape of the engine making it possible to capture all the flow (for maximum M_∞) between the forebody and forebody shock. Second is the rectangular shaped combustor exit which makes possible the use of an aircraft afterbody for the nozzle (refs. 2, 5, and 8).

In considering the weight of the fully rectangular engine module, one important aspect is the fact that the internal surfaces of the engine are formed by flat panels which lead to relatively high structural weights in order to keep panel deflection down. Surfaces with circular or almost circular cross section can be significantly lighter. In fact, preliminary engine weight estimates (by L. R. Jackson of Langley) for a large-scale (89-inch-high) version of the fully rectangular engine module as compared with a similar engine but with a circular combustor, revealed as much as a 28 percent total weight differential. These weight estimates are preliminary in nature, but they still suggest a possibility of considerable weight savings and the potential to operate at higher flight dynamic pressures. Therefore, it becomes desirable to consider a new engine design with a rectangular capture and exhaust area, but with circular internal cross sections, or at least a combustor with essentially circular cross sections. It is desirable to accomplish this weight savings without a penalty in performance.

A conceptual design has been completed for such a new scramjet engine concept (figure 1) labeled the "Rectangular Capture Area to Circular Combustor Scramjet Engine". This new concept has a projected capture area (on a plane normal to the vehicle's forebody surface) which is rectangular in shape (figure 1(b)) with a center body which has a 20° included angle cone followed by a constant diameter cylinder (figure 1(c)). The inlet leading edges are, in general, swept from the engine top to cowl (figure 1(a)) with what are called notches in all leading edges. The design of the inlet inner surface allows for transformation of the rectangular capture area at the inlet entrance into an almost circular cross section (projected on a plane normal to the center body axis) in the strut region. The combustor passes from the almost circular cross-sectional shape of the strut region to a circular shape at the

combustor exit (projected on a plane normal to the centerbody axis). The internal portion of the nozzle includes a transition section from the circular shaped combustor exit back to a rectangle, which makes it relatively easy to use the aft portion of the vehicle as part of the nozzle. The fuel struts, which are located in a radial array at the throat of the inlet and at the entrance of the combustor, pass from the center body to the inlet inner surface and are swept from center body to the inlet inner surface (figure 1(c)). Adjacent struts are staggered relative to each other so that the leading edges lie in a surface which is swept from the engine top to the cowl to facilitate flow spillage through a hole in the cowl during inlet start and normal operation.

Because the cross-sectional shape of the combustor has changed from rectangular to circular, it becomes also necessary to consider the combustor design in conjunction with a new inlet (or engine) design. Therefore, a discussion of the new scramjet engine design is presented which includes a detailed discussion of inlet, strut and combustor designs. Also included are comparisons of some important engine characteristics of the new concept with the like features of the rectangular combustor engine.

SYMBOLS

A	area
G	gap between struts in the inlet throat
H	inlet entrance height
L	combustor length
L_s	length of inlet flow spillage hole
ℓ	the distance in the direction of the inlet entrance flow measured from a line which joins the midpoints of the constant geometry inner surface in the region where the struts intersect the inner surface.
m	mass flow
M	Mach number
p	static pressure
R	radius (figs. 2(a) and 2(b))
T	static temperature
U	flow velocity

W	inlet entrance width
W_s	width of inlet flow spillage hole
x	coordinate parallel to inlet entrance flow (fig. 2(b))
X'	most forward axial point of two adjacent struts being considered
X''	midpoint of constant geometry inner surface in the region where the struts intersect the inner surface
y	vertical coordinate perpendicular to inlet entrance flow (fig. 2(a))
z	horizontal coordinate perpendicular to inlet entrance flow (fig. 2(a))
β	angle defined in figure 2(a)
δ^*	displacement thickness
ρ	density flow
ϕ	fuel equivalence ratio
ϕ_B	fuel equivalence ratio of fuel burned
η_c	combustion efficiency

Subscripts

c	cowl
L.E.	inlet leading edge
S	inlet spillage
T	total
∞	free stream
1	inlet entrance station
2	inlet throat or combustor entrance station
3	combustor exit station

ENGINE DESIGN

The annular shape of the cross sectional area between the forebody shock and a typical vehicle's forebody suggests that a scramjet engine module's capture area should be rectangular in shape. To keep combustor cooling requirements at a reasonable level, multiple, instream fuel struts should be utilized. In order to take advantage of predicted engine weight savings, the combustor should have a circular cross section. The manner in which these three desirable engine design characteristics are incorporated into an engine are discussed in the following sections in terms of inlet design and combustor design.

Inlet Design

The inlet design has two parts: first, the transition section which transforms the rectangular capture stream tube into a cross section which is almost circular; and second, the fuel injection struts.

Transition Section

A review of references 9 through 14 suggests the use of the method of streamline tracing to design the inlet. This method consists of first computing an axisymmetric internal compression field with, for the present design, a conical center body to eliminate the undesirable condition of normal shock waves at the axis of symmetry (using an extension of the analytical techniques of ref. 15). The conical angles of the outer shell and center body as well as the center body size are chosen to limit flow turning angles through the shocks at points where shocks intersect with surfaces to approximately 8° for the incident and 8° for the reflected shocks; this limit of 8° is the result of an attempt to limit boundary-layer separation (ref. 16). The streamlines of the rectangular shaped forebody capture flow (fig. 2(a)) are traced through the conical flow field to the intersection of the leading edge of the fuel struts with the inlet contour (fig. 2(b)). The inlet leading edges are determined from the intersection of the forebody rectangular capture tube with the first compression wave of the axisymmetric flow field at the design Mach number (chosen to be $M_1 = 6.0$).

The cross-sectional shape, as defined by the streamlines, of the flow remains essentially rectangular in shape through the inlet to the leading edge of the struts (fig. 2(c)). However, for the present engine the cross section at the fuel strut leading edge is modified so as to be an essentially circular cross section. In general, the inlet inner surfaces are defined by first passing a series of planes (at different values of β) through the axis of symmetry of the center body and various points on the inlet leading edge. A straight line is then passed from each of these points on the cowl leading edge to a corresponding point at the station where this plane cuts the circular-type cross section at the strut leading edge.

Using the streamline technique, the flow field (fig. 2) from which the preliminary inlet contour (or transition section) was obtained is generated for a design Mach number of $M_1 = 6.0$ by using an internal cone (radius of $R/H = 0.812$) with a 5° cone angle and a cylindrical center body (radius of

R/H = 0.215) with a 20° included angle cone tip located at X/H = 0.472. All lengths are nondimensionalized by engine height. The rectangular-shaped capture flow stream tube has a width of W/H = 1.019 and is shown in figure 2(a) superimposed on the $M_1 = 6.0$ conical flow field. The streamlines of this rectangular shaped stream tube are then traced through the $M_1 = 6.0$ conical flow field (fig. 2(b)) until a one-dimensional contraction ratio of about 3.0 is accomplished; in the conical flow field this occurs at X/H = 3.474. The capture flow stream tube at the X/H = 3.474 station is essentially rectangular (fig. 2(c)) in cross section ($A/H^2 = 0.330$). All areas are nondimensionalized by the square of the engine height. This rectangular type cross section is then approximated by two slightly offset intersecting circles (fig. 2(c)) but with a slight increase in area ($A/H^2 = 0.355$). The radius of the upper circle is 0.389 and the lower circle is 0.368, and they intersect at $\beta = -16.06°$ and $-163.94°$. Most of this increase in area occurs in the cowl region to alleviate possible high local pressures due to the down-turning of the flow by the inlet's swept leading edges during off-design operation and due to the down-turning of the flow through a spillage hole which is to be located in this region. This almost circular cross-sectional shape is swept (in a manner to be discussed along with strut design) and becomes the projected contour of the inlet surface at the strut leading edge.

The inlet leading edges are defined as illustrated in figures 2(a), (b), and (d). For example, from figure 2(a) point A on the rectangular capture flow shape corresponding to $\beta = 51.1°$ has a radius in the conical flow field of R/H = 0.812 and a corresponding Y/H of 0.632. From figure 2(b) it can be seen that the initial shock at R/H = 0.812 from the axis of symmetry is at X/H = 0.0755. A similar procedure for point B with $\beta = 0°$ shows R/H = 0.510, Y/H to be zero and X/H to be 1.357. Repeating the procedure for point C with $\beta = -35.84°$ gives R/H = 0.629, Y/H of -0.368 and X/H of 0.848. These three leading-edge points are on the side wall leading edge and are shown plotted in figure 2(d). The off set of the rectangular capture stream tube from the bottom of the conical flow field (shown in fig. 2(a)) results in the general sweep type nature of the inlet leading edges from engine top (point A) to cowl (point B) as shown in figure 2(d). The turning angle of the flow by a shock at the point where the shock intersects with a surface is shown in figures 3(a) (for $M_1 = 4$) and 3(b) (for $M_1 = 6$) to be less than 8° (weak shock turning) in order to limit boundary-layer separation.

As mentioned before, the internal contour of the inlet is defined by passing a series of planes (at different values of β) through the axis of symmetry of the center body and various points on the inlet leading edge. Where each plane cuts the swept near circular cross section along the strut leading edges, a straight line is passed from the cowl leading edge point to the corresponding point at the strut leading edge. This procedure is used to define the inlet's internal contour for all values of β except for those within about 10^0 of the corners. In the immediate vicinity of the corners the straight line from inlet leading edge to strut leading edge is altered to essentially eliminate any sharp corners in the inlet contour cross sections. The coordinates (β, R/H, X/H, Y/H, and Z/H) of the lines from inlet leading edge to strut leading edge used to define the inlet's internal contour are

presented in Table I. A comparison is presented in figure 4 of a portion of these longitudinal cross-sectional inlet lines with the corresponding cross-sectional lines generated by following the rectangular capture stream tube through the conical flow field.

The size of the spillage hole is governed by the requirement that the present engine have approximately the same spillage schedule as a function of M_1 as the Langley scramjet engine module. For $M_1 = 4.0$ reference 4 shows that 23 percent of the possible capture flow is spilled by that inlet. The size of the spillage hole for the present design is approximated by balancing the pressure and flow direction between internal and external flows at the forward lip of the spillage hole. The external Mach number is 4.0 and the distribution of the Mach number and pressure ratio on the internal surface of the cowl (on the $\beta = -90°$ plane) is presented in figure 5. The arithmetic average of the highest and lowest values of the internal Mach number distribution presented in figure 5 is 2.78 and the pressure ratio corresponding to a Mach number of 2.78 is 5.54. In matching the pressure ratio and flow direction at the forward lip of the spillage hole, the internal flow has to be subjected to an expansion fan and the external flow has to be subjected to a compression. Subjecting the internal flow to an expansion fan of 10° gives a pressure ratio of $P/P_1 = 2.53$ and a downward flow direction toward the cowl of 10°. Subjecting the external flow at the spillage lip to a shock with 10° turning gives a pressure ratio of $P/P_1 = 2.50$ and a downward flow direction from the cowl of 10°. The width of the spillage hole is taken as $W_S/H = 0.78$. Therefore, its length is given by:

$$\left(\frac{L_S}{H}\right) = \frac{0.23\, A_{c/H}{}^2}{\left(\frac{W_S}{H}\frac{(\rho\mu)_S}{(\rho\mu)_1}\right)(\sin 10°)} = 0.94 \qquad 1(a)$$

Where $A_{c/H}{}^2$ is the nondimensionalized capture area (value of 1.019) and W_S/H is the nondimensionalized width of the spillage hole. The mass flow per unit area ratio is given by:

$$\frac{(\rho\mu)_S}{(\rho\mu)_1} = \frac{M_S}{M_1}\left(\frac{T_S}{T_1}\right)^{1/2}\frac{\rho_S}{\rho_1} = 1.79 \qquad 1(b)$$

$M_S = 3.29$

$M_1 = 4.0$

$$\frac{T_S}{T_1} = 1.33$$

$$\frac{\rho_S}{\rho_1} = 1.89$$

The ratios of the spillage parameters to the station 1 parameters correspond to the ratio across a 10° oblique shock with upstream Mach number of 4.0. A similar type of calculation for the case where $M_1 = 6.0$ revealed the hole for $M_1 = 4.0$ to be the larger. It must be pointed out that this is a very approximate method and the correct size of the spillage hole for inlet starting and operation will have to be determined experimentally.

Strut Design

The strut design chosen satisfies three inlet aerodynamic requirements, a structural requirement, and a combustor wetted area requirement. Essentially, the procedure followed in obtaining a satisfactory strut cross section and strut configuration consisted of first satisfying the inlet aerodynamic requirements and then checking to determine if the remaining strut design requirements are satisfied. The inlet aerodynamic requirements of the strut design pertain to the value of the throat Mach number at a design Mach number $M_1 = 6.0$, the swept shock detachment schedule as a function of Mach number M_1 and the minimum strut leading edge Mach number for which supersonic flow could be established between two adjacent struts.

It is assumed that both the Mach number in the throat of the inlet at a design Mach number of $M_1 = 6.0$ and the swept shock detachment schedule as a function of inlet entrance Mach number should be approximately the same as that of the Langley scramjet engine module. The throat Mach number and the shock detachment schedule for the Langley scramjet engine module (refs. 4 and 7) is:

(1) For $M_1 = 6.0$ all shocks are attached

(2) For $M_1 = 4.6$ the third shock inside the struts is detached

(3) For $M_1 = 4.0$ the second shock inside the struts is detached

(4) For $M_1 = 3.0$ the strut leading edge shock is detached

It is felt that the strut leading edge included angle should not be less than 12° (6° half angle) otherwise, the strut will become too thin structurally. The approximate matching of the design throat Mach number and the shock detachment schedule are a function of the strut leading-edge Mach number, strut leading-edge compression angle and the sweep of the strut.

Typical distributions of Mach number as a function of radius, generated for the present engine by conical flow computations in the region of the strut leading edges, are presented in figure 6 for M_1 values of 4.0 and 6.0. The maximum and minimum Mach number of the flow at the strut leading edge are presented in figure 7 as a function of inlet entrance Mach number. It is assumed that the strut leading-edge Mach number of the present engine is equal to the arithmetic average of the high and low values of figure 7. The maximum strut sweep angle is presented in figure 8 as a function of strut leading-edge Mach number, strut leading-edge half angle, and the number of the shock for which swept shock detachment occurred. The case for a strut leading-edge included angle of 12° shows swept shock attachment present up to a sweep angle of 60° for $M_1 = 6.0$. For $M_1 = 4.6$ and a strut leading-edge angle of 12°, swept shock detachment occurs for the second shock between the struts for sweep angle above about 53.5°; therefore shock detachment for a third shock would definitely occur. For $M_1 = 4.0$ and an included angle of 12°, shock detachment occurs for the second shock between the struts for sweep angles above about 50°. For $M_1 = 3.0$ and an included angle of 12°, leading-edge shock detachment occurs for sweep angles above about 48°. Therefore, based on these observations of the theoretical results presented in figure 8, the strut leading-edge sweep angle would be chosen to be 54° for a strut leading edge included angle of 12°. At the engine design Mach number of $M_1 = 6.0$, the assumption of a strut leading edge included angle of 12° and a strut leading-edge sweep angle of 54° produces a throat Mach number of 3.3 (with a strut leading edge Mach number of 4.2) as compared with the throat Mach number 3.4 to 3.5 (with the strut leading-edge Mach number 4.54 to 5.18) for the rectangular combustor engine module. A better comparison between the throat Mach numbers could be obtained by the reduction of the strut leading-edge included angle below the value of 12° but as already pointed out, 12° is considered a lower limit.

The remaining inlet aerodynamic requirement imposed on the strut section and strut configuration design is that it be possible to establish supersonic flow between two adjacent struts for strut leading-edge Mach numbers of 2.5 (approximate $M_1 \approx 4.0$ or greater) or greater; this imposes a maximum one-dimensional contraction ratio of 1.31 or less for the bay between any two adjacent struts. The one-dimensional contraction ratio between any two adjacent struts is a function of the strut sweep, included angle, length to chord, stagger or displacement (axial) relative to adjacent struts as well as the number of struts. The strut sweep and included angle have been chosen to be 54° and 12°, respectively. With these quantities specified, the strut length to average chord length becomes a function of strut stagger or displacement (axial) and the number of struts. The circumferential distribution of the strut leading edges around the center body is determined by dividing 360° by the number of struts. Each strut, starting with the top center strut to the bottom center strut, is displaced axially from an adjacent strut by a distance equal to the chord length of a sector of the center body cross section of angle 360° divided by the number of struts. Only even numbers of struts were evaluated because an odd number of struts results in there being two bottom struts (in the cowl region) located at the same axial location. For a 24 strut assumption, typical cross-sectional strut shapes at the intersection with the center body

are presented in figure 9(a). Also, for the 24 strut assumption typical cross-sectional shapes are presented in figure 9(b) for the longest struts at R/H = 0.234 from the center body. Shorter struts are obtained by cutting off the longest struts to the appropriate lengths. The forward section of this strut example and all other examples considered, are determined by shocks similar to those shown. The shocks pass from the leading edges of two adjacent struts to the surface of the adjacent strut where it is cancelled by the turning of the surface. For both sides of the top center strut and the lower surface of all other struts, except the bottom center strut, the line on the strut surface from outer shell to center body defined by the intersection of the swept shock becomes the throat between any two adjacent struts, and a step is placed at this point in the strut surface for injector location.

Detailed computations for the axial variation of the one-dimensional contraction ratio between two adjacent struts were made for a 16 strut assumption and the results are presented in figure 10. For struts in the top half of the scramjet throat and without an injector step, i.e., struts with the larger ratio of strut length to chord length, the maximum one-dimensional contraction ratio is shown in figure 10 to be about 1.36. The same struts, but with injector steps, are shown to result in a maximum one-dimensional contraction ratio of 1.27. For struts with an injector step and in the lower half of the scramjet throat, i.e., struts with the smaller ratio of strut length to chord length, the maximum one-dimensional contraction ratio is shown in figure 10 to be about 1.36. If the outer shell has a 3° expansion instead of constant area beginning at the strut leading edges as well as the injector step, the maximum one-dimensional contraction area is shown in figure 10 to reduce to about 1.27. It is desirable not to have the 3° outer shell expansion, and in order to eliminate the need for the expansion the number of struts has to be increased, which in turn increases the ratio of strut length to chord length. For the case with 24 struts the maximum one-dimensional contraction ratio for struts in the lower half of the engine is shown in figure 10 to be about 1.31; a maximum one-dimensional contraction ratio of 1.31 was specified initially as the maximum desirable one-dimensional contraction ratio between the struts. The strut configuration chosen consists of 24 struts whose leading edges are staggered in the manner indicated in figure 9(c). The coordinates of the intersection of the strut leading edges with the inlet's internal surface are presented in Table II. The ratio of strut length to average maximum thickness is between 5.6 and 6.6, which is felt to be a structural improvement over the Langley scramjet engine module. The remaining strut design requirement, the one pertaining to combustor wetted area, will be discussed in a following section on combustor design.

Inlet Wetted Surface Area

Based on the inlet transition section, strut shape, and strut confifuration as presented, the ratio of inlet internal wetted surface area (neglecting spillage hole) to capture area is given by:

$$\frac{A_{\text{Inlet Wet}}}{A_c} = \left[\left(\frac{A_{\text{inner surface}}}{A_c}\right) + \left(\frac{A_{\text{center body}}}{A_c}\right) + \left(\frac{A_{\text{strut}}}{A_c}\right)\right]_{\text{wetted}} \tag{2}$$

$$= 10.67 + 4.01 + 1.99 = 16.67$$

From reference 3 the ratio of inlet internal wetted area to capture area of the Langley scramjet engine module is approximately 13.0.

Combustor Design

The main restrictions on the combustor design are that it be essentially circular in cross section, have an area ratio of 4.0 for M_∞ between 5.5 and 7.5, have an area ratio of 5.0 for M_∞ below 5.5 (ref. 2), and a minimum of combustor wetted surface area. The combustor of the present engine is designed to have an essentially circular cross-sectional area at the trailing edge of the struts and becomes a circular section at the combustor exit.

The development of a combustor which has good performance over a free-stream Mach number range requires the careful tailoring of schedules of combustor area versus length with schedules of fuel burned versus length such that thermal choking does not occur over the Mach number range at any point in the combustor. In order to develop a viable combustor design, it is necessary to specify the inlet mass flow spillage, inlet aerodynamic contraction ratio, and, for combustor length determination, the gap between the struts. For the design of the present engine it is assumed that the inlet mass flow spillage and aerodynamic contraction ratio follow the same schedule as a function of M_1 as that for the Langley scramjet engine module; in the finalized design the values of these two inlet parameters will have to be determined experimentally. The physical gap between the struts varies from $G/H = 0.031$ at the strut intersection with the center body to $G/H = 0.063$ at the intersection with the outer shell; the arithmetic average value for G/H is 0.047.

A two point combustor design was chosen; that is, designed to be exactly applicable to two Mach numbers. The combustor designed for the Langley Scramjet modular engine was designed for $M_\infty = 6.0$ ($M_1 = 5.58$) and $M_\infty = 4.0$ ($M_1 = 3.54$); for comparison purposes, point designs for the present engine will be developed and presented for the same Mach numbers. For $M_\infty = 6.0$, it is assumed (from ref. 4) that the inlet aerodynamic contraction ratio is 7.08 and spillage is 8.1 percent. For $M_\infty = 4.0$, it is assumed (from ref. 4) that the inlet aerodynamic contraction ratio is 4.05 and spillage is 32 percent. The aerodynamic throat area is given by,

$$\frac{A_2}{H^2} = \frac{\left(\frac{m_1}{m_c}\right)\left(\frac{A_c}{H^2}\right)}{\frac{A_1}{A_2}} \tag{3}$$

For $M_\infty = 6.0$, $M_1 = 5.58$,

$$\frac{A_2}{H^2} = \frac{(1 - 0.08)\ (1.02)}{7.08} \tag{4}$$

$$\frac{A_2}{H^2} = 0.13$$

For $M_\infty = 4.0$, $M_1 = 3.54$,

$$\frac{A_2}{H^2} = \frac{(1 - 0.32)\ (1.02)}{4.05} \tag{5}$$

$$\frac{A_2}{H^2} = 0.17$$

For $M_\infty = 6.0$ the nondimensionalized combustor exit area is given by,

$$\frac{A_3}{H^2} = 4.0\ \frac{A_2}{H^2} \tag{6}$$

$$\frac{A_3}{H^2} = 0.53$$

For $M_\infty = 4.0$ the nondimensionalized combustor exit area is given by,

$$\frac{A_3}{H^2} = 5.0\ \frac{A_2}{H^2} \tag{7}$$

$$\frac{A_3}{H^2} = 0.86$$

Knowing the combustor exit areas (eqs. (6) and (7)) for the $M_\infty = 6.0$ and 4.0 cases, an area variation as a function of fuel burned, ϕ_B, which does not produce combustor choking must be developed. This is accomplished through use of an altered form of the engine performance method of reference 4. This altered form allows for step computations in terms of area and ϕ_B through the combustor as well as an approximate means for accounting for higher stream tube surface pressures (or forces) in the vicinity of the injectors. Upon obtaining a schedule of area versus ϕ_B, which does not produce choking, a realistic schedule of physical area versus length must be developed. This is accomplished through use of the relationship between the combustion efficiency, η_c, versus ℓ/L and the relationship between the fuel burned and η_c given by,

$$\phi_B = \eta_c \phi \tag{8}$$

The parameter ℓ is the axial distance along the combustor measured from a line which joins the midpoints of the constant inner surface geometry section in the region where the struts intersect the inner surface and L is the total combustor length.

A nondimensionalized area variation, which does not produce combustor choking is presented in Tables III and IV as a function of ϕ_B for $M_\infty = 6.0$ and 4.0, respectively. In the engine performance computations, the fuel was injected in two steps, $\phi = 0.3$ normal to the flow, and $\phi = 0.7$ parallel to the flow to give a total fuel injected corresponding to $\phi = 1.0$. Combustion efficiency at the combustor exit is assumed to be 0.95 for $M_\infty = 6.0$ and 0.8 for $M_\infty = 4.0$. It is assumed (ref. 17) that the combustor length is given by,

$$L = 50\,(G - \delta^*) \tag{9}$$

which would result in lengths for $M_\infty = 6.0$ and 4.0 that differ by a small amount (due to differing displacement thicknesses, δ^*). For the present design, it is assumed that δ^* is zero and the length of the combustor becomes 50 times the average physical gap (which gives conservative combustor length). Since this result produces the dilemma of two areas (eqs. (6) and (7)) at the same combustor length, it is then assumed that controls on combustion can be imposed so as to reduce total combustor length by 1/3 for $M_\infty = 6.0$ (to 33.3 G/H or L/H = 1.57) and increase total combustor length by 1/3 for $M_\infty = 4.0$ (to 66.7 G/H or L/H = 3.14). It is felt that this can be accomplished by controlling the split between parallel and normal injection of the fuel. For the present combustor design, it is assumed for $M_\infty = 6.0$ the normal injection ϕ is 0.3 and parallel injection is 0.7 and for $M_\infty = 4.0$ the normal injection

is between 0 and 0.1, and the parallel injection between 0.9 and 1.0. Based on these assumptions the distribution of combustion efficiency, η_c, as a function of ℓ/L for $M_\infty = 6.0$ and 4.0 is assumed to be similar to those presented in figure 11 (suggested from cold mixing data, ref. 17). A realistic schedule of fuel burned ϕ_B versus ℓ/L is then generated by combining the curves of η_c versus ℓ/L of figure 11 with equation (8) and the respective total combustor lengths for $M_\infty = 6.0$ $(L/H = 1.57)$ and $M_\infty = 4.0$ $(L/H = 3.14)$. Upon combining the schedules of ϕ_B versus area from Tables III and IV with the respective ϕ_B versus ℓ/L schedules generated from figure 11, a schedule of area versus ℓ/L for which combustor choking does not occur is obtained. The results obtained from these computations are presented in Tables V and VI.

In defining the physical combustor area variation with length it is specified that the areas and axial locations for the exit stations for $M_\infty = 6.0$ and 4.0 are to be exactly matched with those for which combustor choking does not occur at any point. The combustor entrance is assumed to occur along a line which is located at the midpoint of the inner surface constant geometry section. This is at a distance of $\Delta X/H = 0.27$ from the line of the strut leading edge as given in Table I. The line which defines the combustor exits on the engine inner surface is $L/H = 1.57$ (for $M_\infty = 6.0$) and $L/H = 3.14$ (for $M_\infty = 4.0$) from the line which defines the entrance (Table I) on the engine inner surface. The outline of the $M_\infty = 6.0$ and $M_\infty = 4.0$ combustor exits projected on a plane normal to the center-body axis are circular and offset so that a point on the innerbody surface at the $\beta = -90^\circ$ plane has a value of $Y/H = -0.368$. Thus, the center of the projected circle for the combustor exit for $M_\infty = 6.0$ is on a line $Y/H = 0.042$ in the $\beta = 90°$ plane and has a radius of $R/H = 0.41$. The center of the projected circle for the combustor exit for $M_\infty = 4.0$ is on a line $Y/H = 0.16$ in the $\beta = 90°$ plane and has a radius of $R/H = 0.52$. The combustor exit lines on the inner surface of the engine are presented in Table I in terms of X/H and R/H for $M_\infty = 6.0$ and $M_\infty = 4.0$. The physical area distribution as a function of ℓ/L is presented in figure 12 and also in Tables V and VI.

Combustor Wetted Surface Area

The center-body combustor wetted area is approximated corresponding to the assumption of a conical shaped trailing edge which begins along a line $\Delta X/H = 0.53$ down stream of the line defined by the strut leading-edge intersections with the center body. For computational purposes the angle between the cylindrical portion of the center body and the conical section was chosen to be 10°.

The ratio of combustor surface wetted area to the cowl area is given by,

$$\frac{A_{comb.\ w.}}{A_c} = \left[\left(\frac{A_{strut}}{A_c}\right) + \left(\frac{A_{inner\ surface}}{A_c}\right) + \left(\frac{A_{center\ body}}{A_c}\right)\right]_{Wetted} \tag{10}$$

For $M_\infty = 6.0$ and $M_1 = 5.58$,

$$\frac{A_{comb.\ w.}}{A_c} = 0.75 + 3.91 + 0.96 = 5.62$$

For $M_\infty = 4.0$ and $M_1 = 3.54$,

$$\frac{A_{comb.\ w.}}{A_c} = 0.75 + 8.43 + 0.96 = 10.14$$

It is pointed out above that a combustor has also been designed for the Langley scramjet engine module using essentially the same procedure. In comparison, the combustor for the Langley scramjet engine module has a ratio of combustor wetted area to cowl area of approximately 7.6 for $M_\infty = 6.0$ and $M_1 = 5.58$ and a value of approximately 12.86 for $M_\infty = 4.0$ and $M_1 = 3.54$.

CONCLUDING REMARKS

A concept for a new scramjet engine design is presented. This engine has a projected capture area which is rectangular in shape with a center body which has a 20° included angle cone followed by a constant diameter cylinder. The inlet leading edges are, in general, swept from top to cowl with notches in each. The method of design of the inlet inner surface is that of streamline tracing. The inlet transforms the rectangular capture stream tube into a cross section which is almost circular in shape at the strut leading edges. The high pressure and temperature regions of the combustor are almost circular in shape and, thus, the benefits of hoop stresses in relation to structural weights can be utilized to reduce combustor and engine weights. The fuel struts, which are located in a radial array at the throat of the inlet and at the entrance of the combustor, pass from the center body to the inlet inner surface and are swept 54° from the center body to the inlet inner surface. Strut length to maximum average thickness ratios are between 5.6 and 6.6, which represents a structural improvement over the Langley scramjet engine module. Strut leading edges lie in a plane which is swept from engine top to the cowl to facilitate flow spillage

out through the bottom of the inlet during inlet start and normal operation. Combustor wetted areas are shown to be a function of free-stream Mach number as well as vehicle forebody Mach number. For $M_\infty = 6.0$ and $M_1 = 5.58$, the ratio of combustor wetted area to cowl area of the new engine design is 5.62 as compared to 7.6 for the all rectangular module; for $M_\infty = 4.0$ and $M_1 = 3.54$, the ratio of combustor wetted area to cowl area is 10.14 as compared to 12.86. This decrease in combustor wetted area is offset somewhat by an increase in inlet wetted area. Fine tuning of the inlet and combustor design can only be accomplished through experimental testing.

REFERENCES

1. Marino, A.; and Schneider, J.: Interrelation Between Scramjet Engine Design, Engine Cooling Requirement and Vehicle-Engine Size Requirement for a Shuttle-Boost Mission. NASA CR-2175, Mar. 1973, General Applied Science Laboratories, Inc., Confidential.

2. Henry, John R.; and Anderson, Griffin Y.: Design Considerations for the Airframe-Integrated Scramjet; NASA TM X-2895, 1973.

3. Pinckney, S. Z.: Turbulent Heat-Transfer Predication Method for Application to Scramjet Engines; Langley Research Center. NASA TN D-7810, Nov. 1974.

4. Pinckney, S. Z.: Internal Performance Predictions for Langley Scramjet Engine Module. NASA TM S-74038, 1977.

5. Becker, John V.: New Approaches to Hypersonic Aircraft. Seventh Congress of the International Council of the Aeronautical Sciences, Rome, Italy, Sept. 1970.

6. Trexler, Carl A.; and Souders, Sue W.: Design and Performance at a Local Mach Number of 6 of an Inlet for an Integrated Scramjet Concept. NASA TN D-7944, Aug. 1975.

7. Trexler, Carl A.: Inlet Performance of the Integrated Langley Scramjet Module (Mach 2.3 to 7.6). AIAA Paper 75-1212, AIAA/SAE 11th Propulsion Conference, Anaheim, Calif., Sept. 29 - Oct. 1, 1975.

8. Wieting, Allan R.; and Guy, Robert W.: Preliminary Thermal-Structural Design and Analysis of an Airframe-Integrated Hydrogen-Cooled Scramjet. AIAA Paper 75-137, AIAA 13th Aerospace Science Meeting, Pasadena, Cal., Jan. 20-22, 1975.

9. Hartill, W. R.: Analytical and Experimental Investigation of a Scramjet Inlet of Quadriform Shape. Technical Rep. AFAPL-TR-65-74, U.S. Air Force, Aug. 1965, Marquardt Corp.

10. Gen. Elec. Co.: Advanced Air-Breathing Engines, Vol, II, Experimental Investigation. Technical Rep. APL-TDR-64-21, U.S. Air Force, May 7, 1964.

11. Anon: Quarterly Review of: Analytical and Experimental Evaluations of the Supersonic Combustion Ramjet Engine. BPSN 4 (6299-615E), (Contract AF33 (615) - 1586), Advanced Engine and Technol. Department, Gen. Elec. Co., Feb. 10, 1965.

12. Gen. Elec. Co.: Analytical and Experimental Evaluation of the Supersonic Ramjet Engine. Vol. III - Component Evaluation. AF APL-TR-65-103, U.S. Air Force, Dec. 1, 1965.

13. Keirsey, J. L.: A Study of the Aerodynamics of Scramjet Engine Inlets. TG-732, Appl. Phys. Lab., Johns Hopkins Univ., Sept. 1965. (Available from DDC as AD370936).

14. Keirsey, J. L.; and Snow, M. L.: Modular Inlet Investigation. Quarterly Report, Aeronautics Division, Research and Development, AQ/66-1, Appl. Phys. Lab., Johns Hopkins Univ., Jan. - Mar. 1966.

15. Salas, Manuel D.: The Anatomy of Floating Shock Fitting; AIAA Journal Vol. 14, no. 5, 1976, pp. 583-588.

16. Pinckney, S. Z.: Semiempirical Method for Predicting Effects of Incident-Reflecting Shocks on the Turbulent Boundary Layer; Langley Research Center, NASA TND-3029, Oct. 1965.

17. Anderson, Griffin Y.; Eggers, James M.; Waltrup, Paul J.; and Orth, Richard C.: Proceedings of the 13th JANNAF Combustion Meeting, Monterey, Calif., Sept. 13-17, 1976.

Table I

Coordinates of Inner Surface of Engine

$\frac{m}{m_T}$	β	Inlet Leading Edge				Region of Constant Projected Geometry: Line of Intersection of Strut Leading Edges with Inlet Inner Surface				Comb. Entrance	Comb. Divergence	Comb. Exit	
		$\left(\frac{R}{H}\right)$	$\left(\frac{X}{H}\right)$	$\left(\frac{Z}{H}\right)$	$\left(\frac{Y}{H}\right)$	$\left(\frac{R}{H}\right)$	$\left(\frac{X}{H}\right)$	$\left(\frac{Z}{H}\right)$	$\left(\frac{Y}{H}\right)$	$\left(\frac{X}{H}\right)$	$\left(\frac{X}{H}\right)$	$M_\infty = 6.0$ R/H = .410 $\left(\frac{X}{H}\right)$	$M_\infty = 4.0$ R/H = .524 $\left(\frac{X}{H}\right)$
.394	0	.510	1.357	.510	0	.385	3.995	.385	0	4.268	4.542	5.833	7.403
.4	6.88	.513	1.340	.510	.0623	.393	3.957	.389	.0472	4.230	4.504	5.795	7.365
.45	20.6	.544	1.212	.510	.193	.406	3.878	.379	.143	4.151	4.425	5.716	7.286
.5	27.38	.574	1.084	.510	.264	.413	3.838	.368	.191	4.112	4.386	5.677	7.247
.6	35.84	.629	.848	.510	.368	.421	3.787	.342	.247	4.061	4.335	5.626	7.196
.7	41.37	.680	.634	.510	.449	.427	3.757	.321	.281	4.030	4.304	5.595	7.165
.8	45.41	.727	.438	.510	.517	—	—	—	—	—	—	—	—
.4	-6.88	.513	1.340	.510	-.0623	.378	4.036	.376	-.0453	4.310	4.584	5.875	7.445
.45	-20.6	.544	1.212	.510	-.193	.368	4.114	.345	-.130	4.387	4.661	5.952	7.522
.5	-27.38	.574	1.084	.510	-.264	.368	4.151	.327	-.170	4.424	4.698	5.989	7.559
.625	80	.642	.793	.111	.632	.447	3.530	.0774	.442	3.808	4.082	5.373	6.943
.606	90	.632	.834	0	.632	.449	3.474	0	.449	3.747	4.021	5.312	6.882
.7	68.47	.680	.634	.249	.632	.446	3.596	.164	.413	3.870	4.144	5.435	7.005
.8	60.48	.727	.438	.359	.632	.442	3.642	.217	.385	3.915	4.189	5.480	7.050
.206	-90	.368	1.369	0	-.368	.368	4.514	0	-.368	4.787	5.061	6.352	7.922
.212	-80	.374	1.850	.0642	-.368	.368	4.478	.0642	-.362	4.751	5.025	6.316	7.886
.236	-68.98	.395	1.784	.142	-.368	.368	4.401	.132	-.344	4.674	4.948	6.239	7.809
.3	-55.91	.446	1.608	.249	-.368	.368	4.323	.206	-.306	4.597	4.871	6.162	7.732
.359	-49.18	.487	1.452	.317	-.368	.368	4.278	.240	-.279	4.551	4.825	6.116	7.686
.4	-45.82	.513	1.340	.359	-.368	.368	4.259	.257	-.264	4.532	4.806	6.097	7.667
.5	-39.9	.574	1.084	.440	-.368	.368	4.227	.283	-.236	4.500	4.774	6.065	7.635
.546	-31.8	.600	.976	.510	.315	.368	4.180	.313	-.194	4.453	4.727	6.018	7.588
.427	-16.06	.530	1.271	.510	-.147	.368	4.087	.353	-.102	4.361	4.635	5.926	7.496
.427	16.06	.530	1.271	.510	.147	.402	3.904	.385	.111	4.178	4.452	5.743	7.313

Straight Line Segments									
$\frac{m}{m_T}$	β	$\frac{R}{H}$	$\frac{X}{H}$	$\frac{Z}{H}$	$\frac{Y}{H}$	$\frac{R}{H}$	$\frac{X}{H}$	$\frac{Z}{H}$	$\frac{Y}{H}$
1.0	51.1	.812	.0755	.510	.632	.719	.840	.451	.561
1.0	51.1	.719	.840	.451	.561	.668	1.340	.419	.521
1.0	51.1	.668	1.340	.419	.521	.606	1.888	.381	.472
1.0	51.1	.606	1.888	.381	.472	.570	2.265	.359	.444
1.0	51.1	.570	2.265	.359	.444	.434	3.698	.274	.338
.9	55.12	.770	.251	.440	.632	.617	1.782	.353	.506
.9	55.12	.617	1.782	.353	.506	.436	3.678	.249	.359
.9	48.56	.770	.251	.510	.578	.610	1.782	.404	.457
.9	48.56	.610	1.782	.404	.457	.542	2.449	.359	.406
.9	48.56	.542	2.449	.359	.406	.432	3.715	.287	.325
.6	-35.84	.629	.848	.510	-.368	.538	1.888	.436	-.315
.6	-35.84	.538	1.888	.436	-.315	.368	4.202	.298	-.215

Table II

Intersection of Strut Leading Edges
with Internal Surface of Inlet

Strut Number	β, Deg	X/H	R/H	Y/H	Z/H
1	90	3.474	.449	.449	0
2	75	3.561	.447	.432	.116
3	105	3.561	.447	.432	-.116
4	60	3.648	.440	.381	.220
5	120	3.648	.440	.381	-.220
6	45	3.736	.429	.304	.304
7	135	3.736	.429	.304	-.304
8	30	3.823	.416	.208	.360
9	150	3.823	.416	.208	-.360
10	15	3.911	.400	.104	.387
11	165	3.911	.400	.104	-.387
12	0	3.998	.384	0	.384
13	180	3.998	.384	0	-.384
14	-15	4.086	.378	-.0978	.365
15	-165	4.086	.378	-.0978	-.365
16	-30	4.173	.368	-.184	.319
17	-150	4.173	.368	-.184	-.319
18	-45	4.260	.368	-.260	.260
19	-135	4.260	.368	-.260	-.260
20	-60	4.348	.368	-.319	.184
21	-120	4.348	.368	-.319	-.184
22	-75	4.435	.368	-.356	.0953
23	-105	4.435	.368	-.356	-.0953
24	-90	4.523	.368	-.368	0

Table III

$M_\infty = 6.0, \quad M_1 = 5.58$

ϕ	A/A_2	ϕ_B	A/H^2
0	1.0	0	.1323
.3	1.25	.075	.1654
1.0	2.50	.33	.3308
1.0	3.0	.54	.3969
1.0	3.5	.74	.4631
1.0.	4.0	.95	.5292

Table IV

$M_\infty = 4.0, \quad M_1 = 3.54$

ϕ	A/A_2	ϕ_B	A/H^2
0	1.0	0	.1725
.3	1.25	.075	.2156
1.0	2.50	.28	.4313
1.0	3.0	.38	.5175
1.0	3.25	.43	.5606
1.0	3.75	.54	.6469
1.0	4.25	.64	.7331
1.0	4.50	.70	.7763
1.0	4.75	.75	.8194
1.0	5.0	.80	.8625

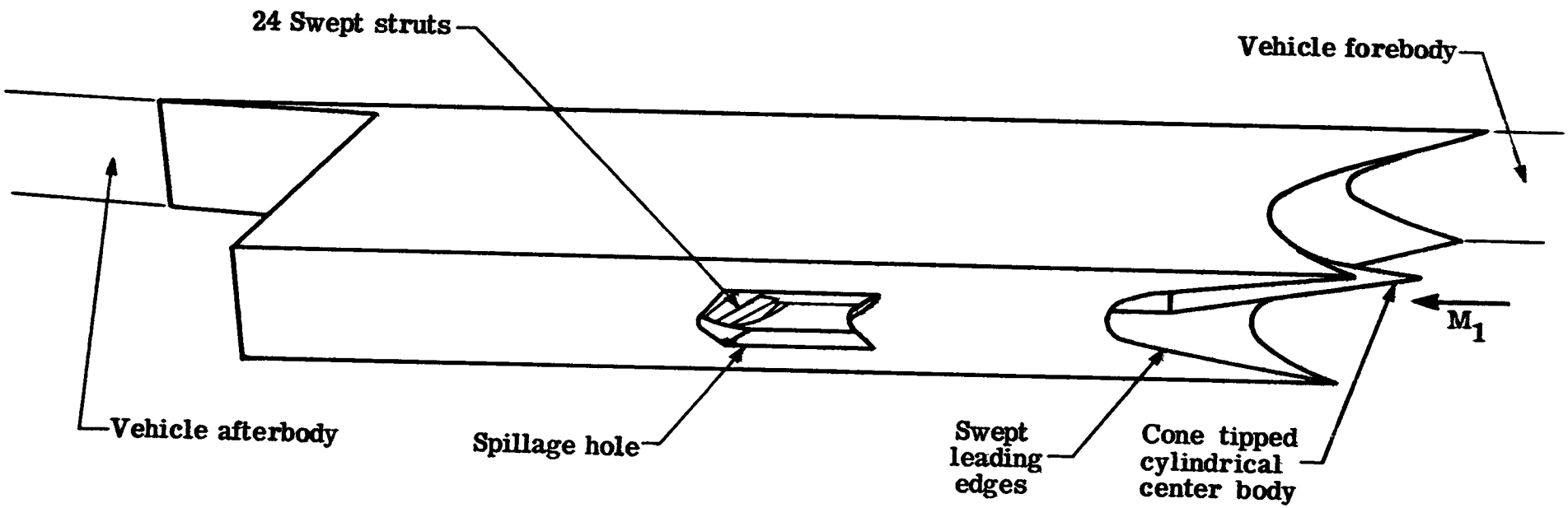

(a).- Side view.

Figure 1.- Perspective view of rectangular capture area to circular combustor scramjet engine.

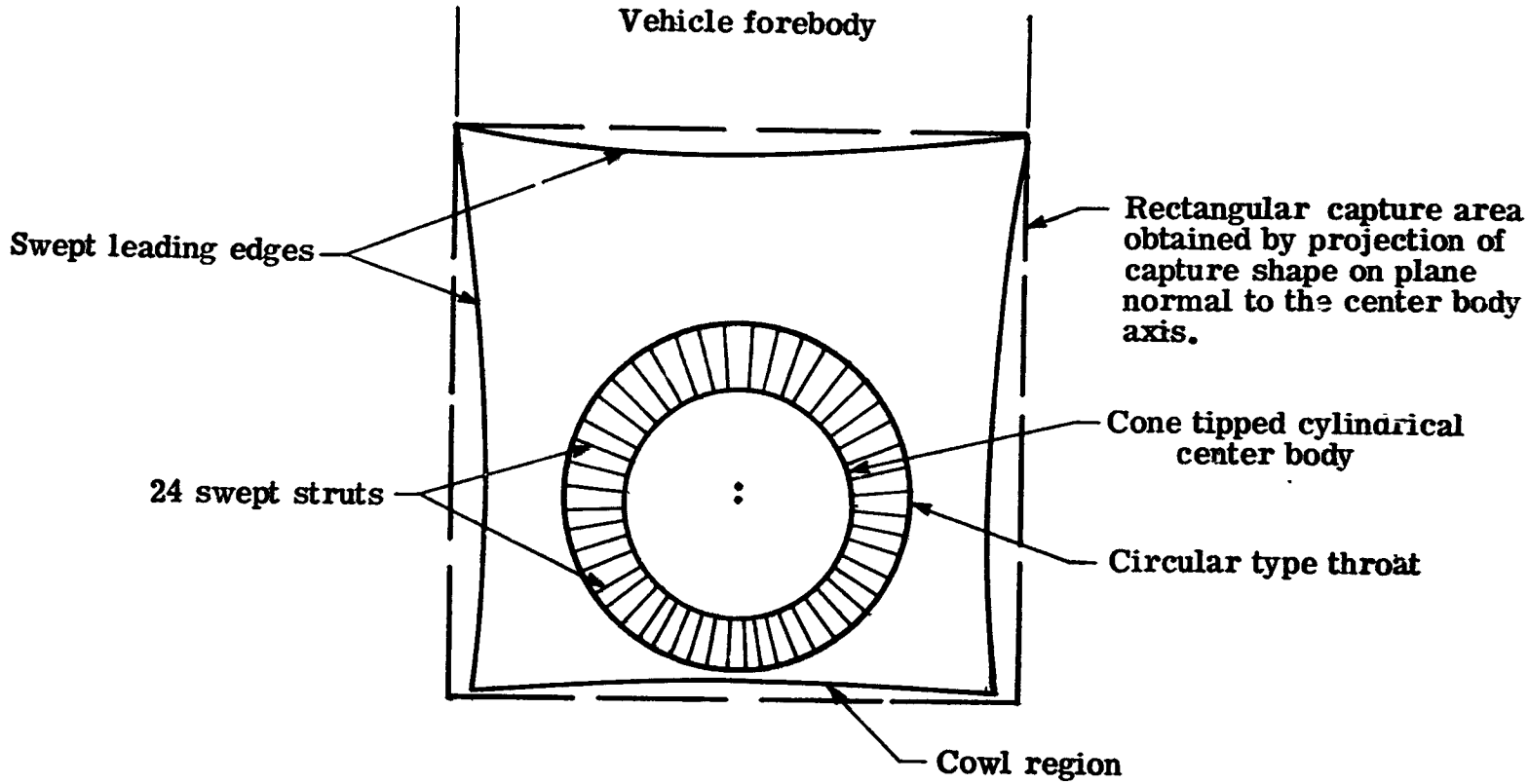

(b).- Frontal view.

Figure 1.- Continued.

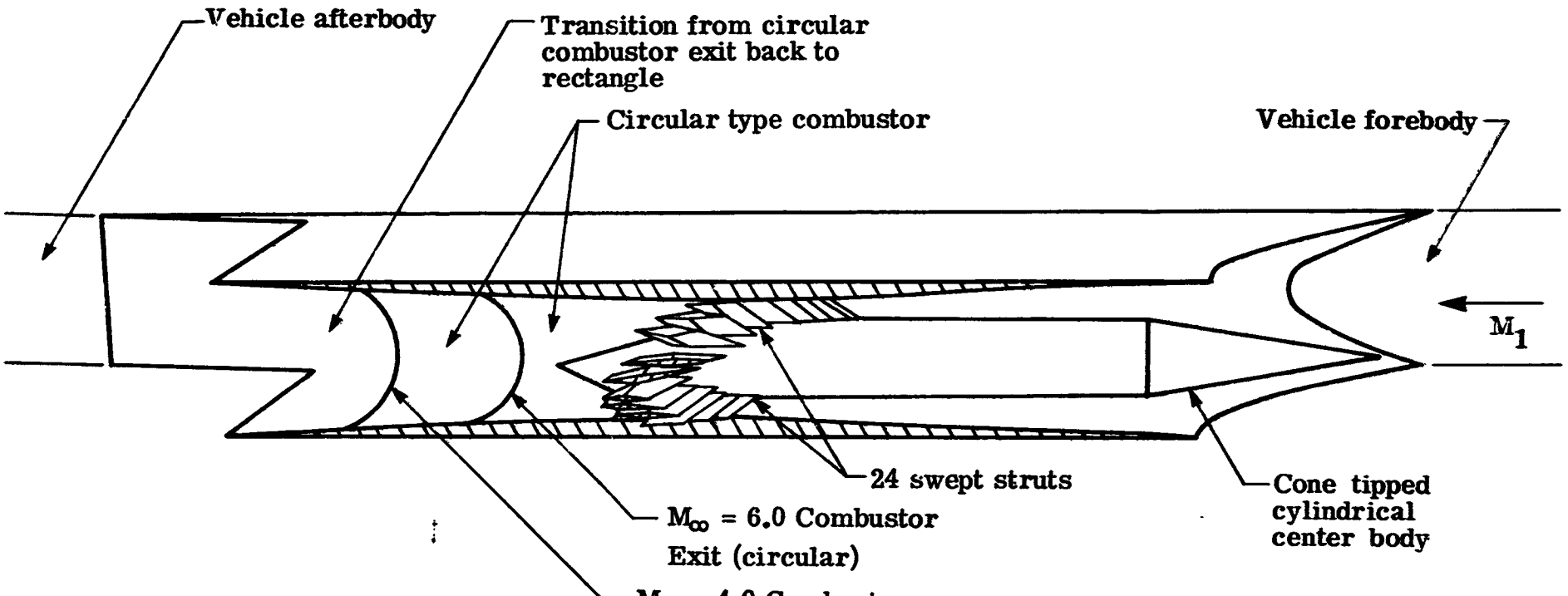

(c).- Cut away view.

Figure 1.- Concluded.

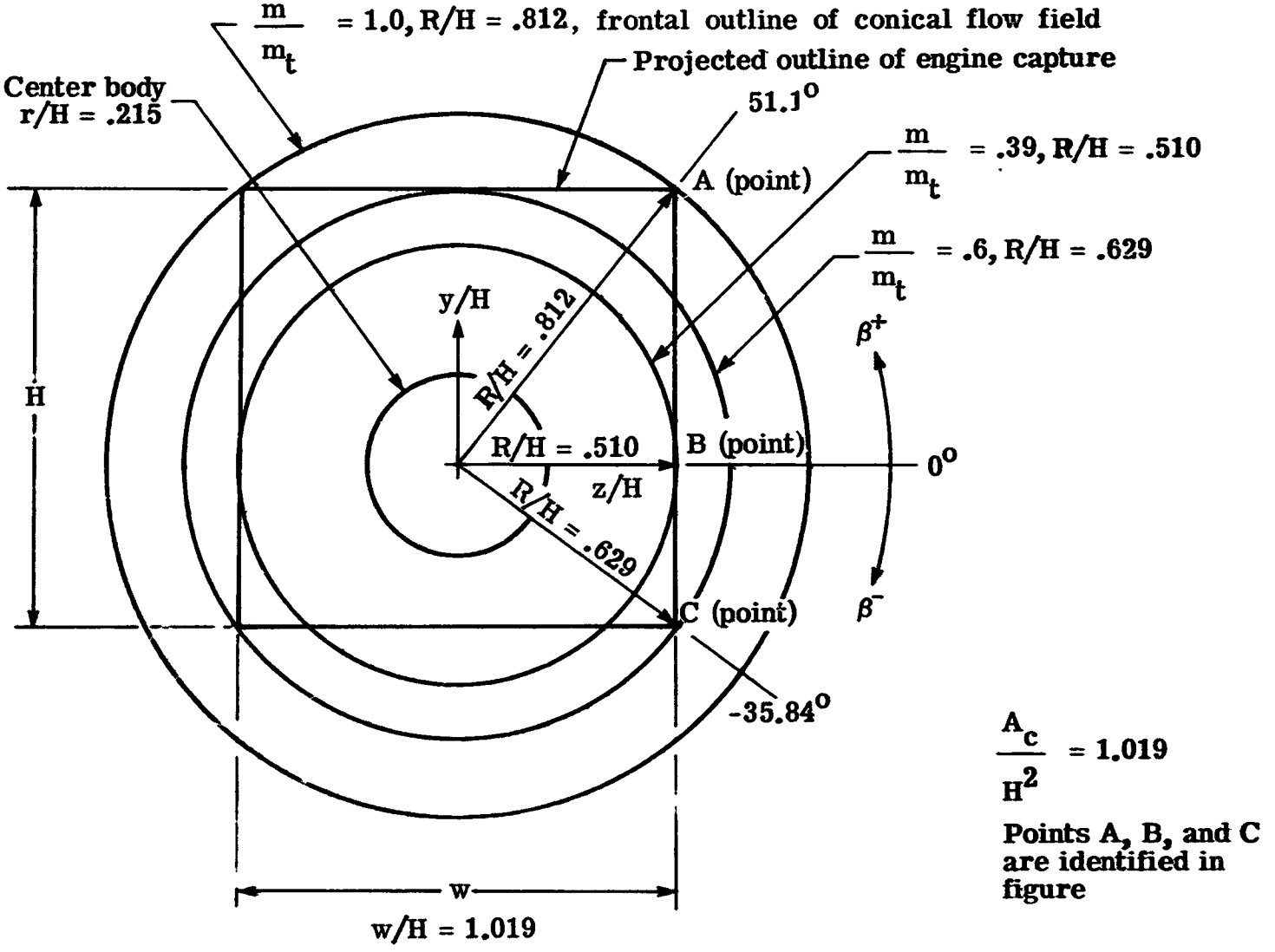

(a).- Engine capture shape.

Figure 2.- Conical flow field relationship with rectangular capture area to circular combustor scramjet engine.

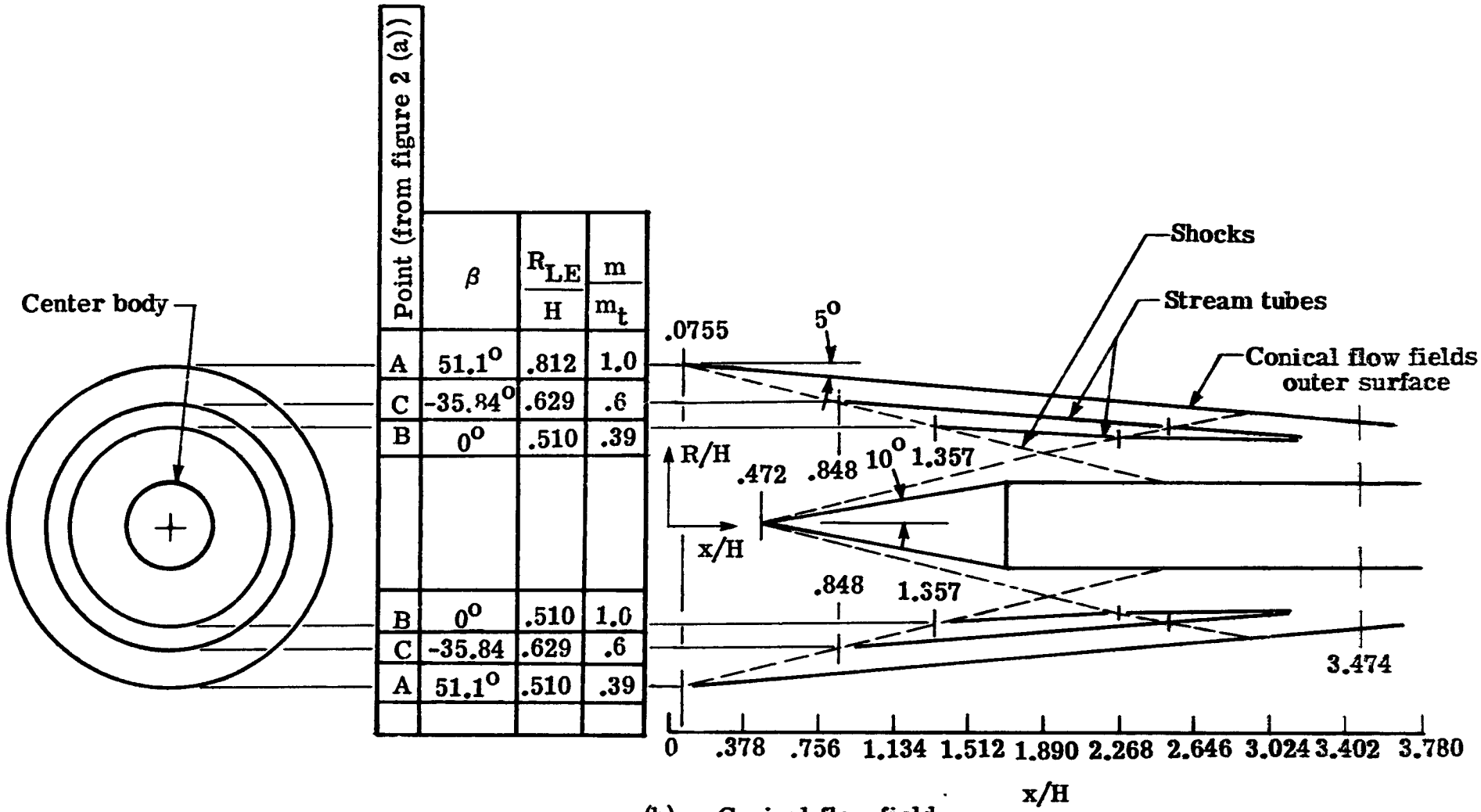

(b).- Conical flow field.

Figure 2.- Continued.

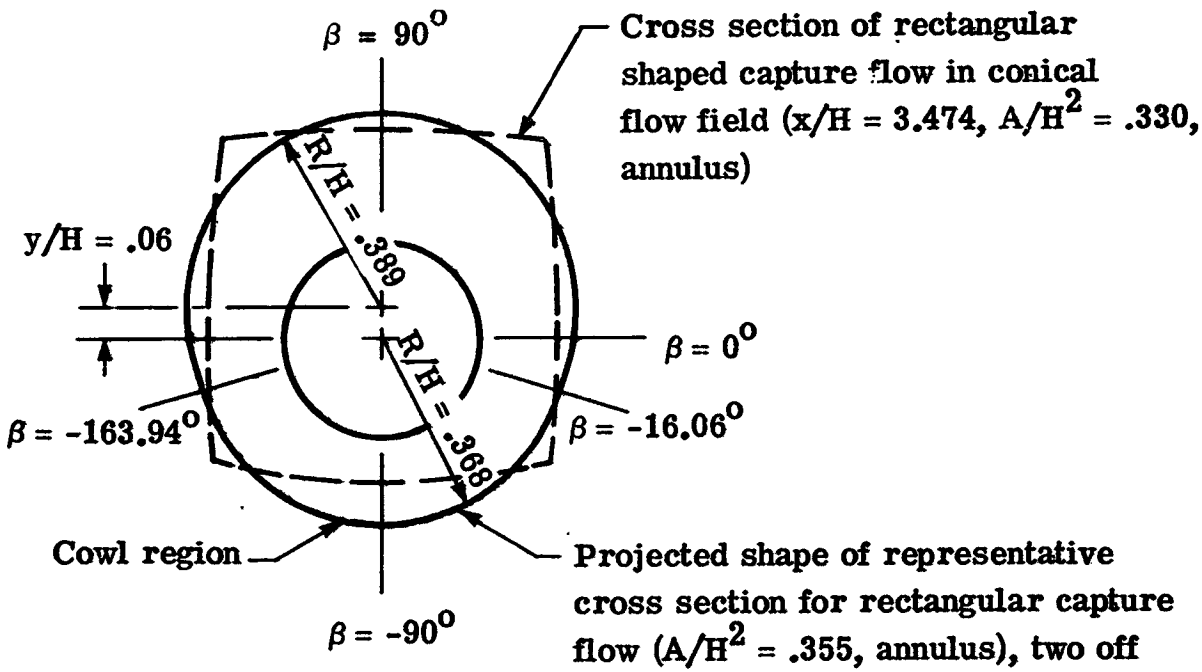

(c).- Inlet inner surface at strut leading edge.

Figure 2.- Continued.

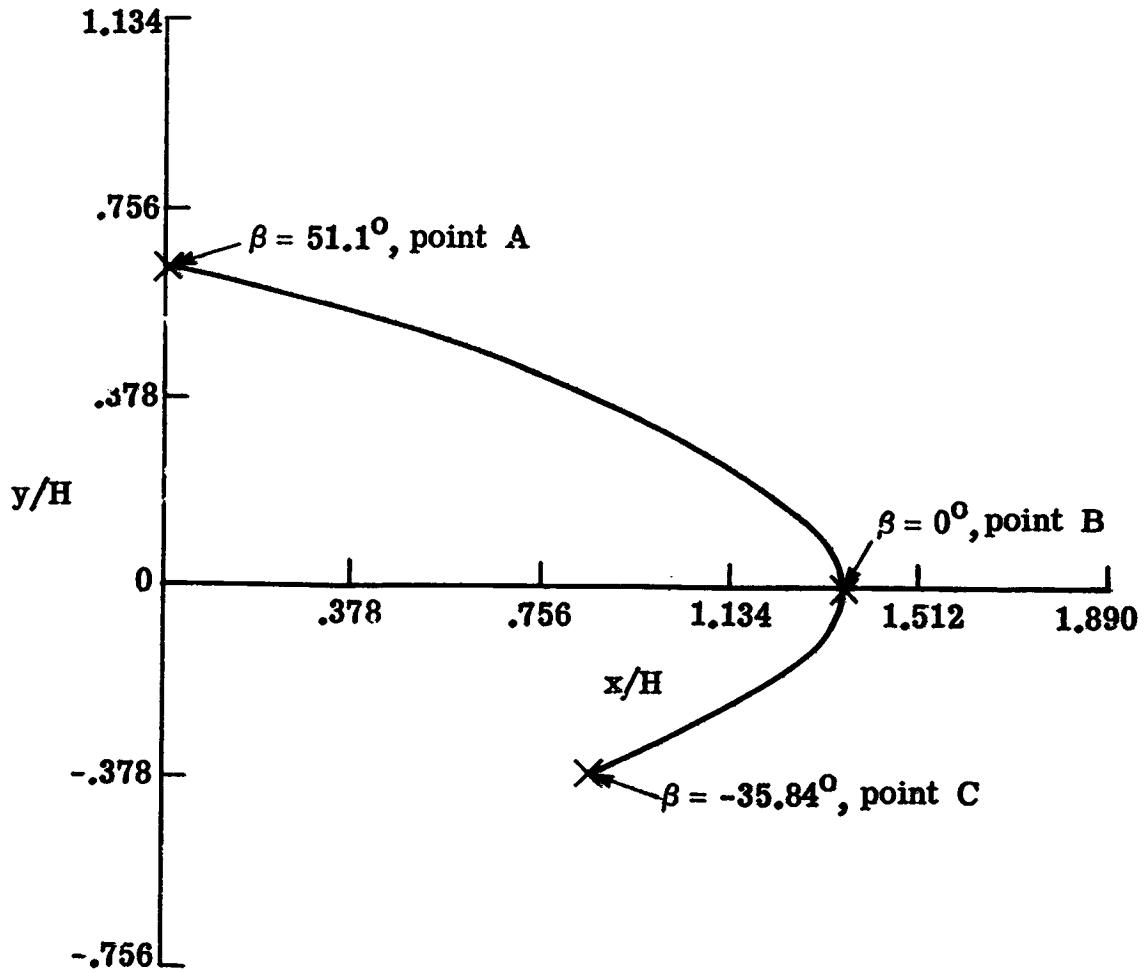

(d).- Side wall leading edge.

Figure 2.- Concluded.

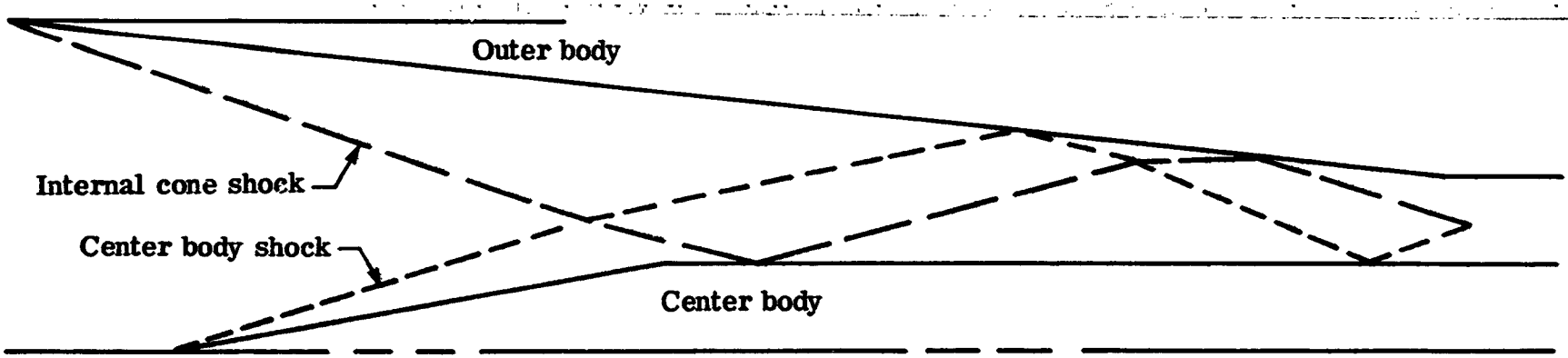

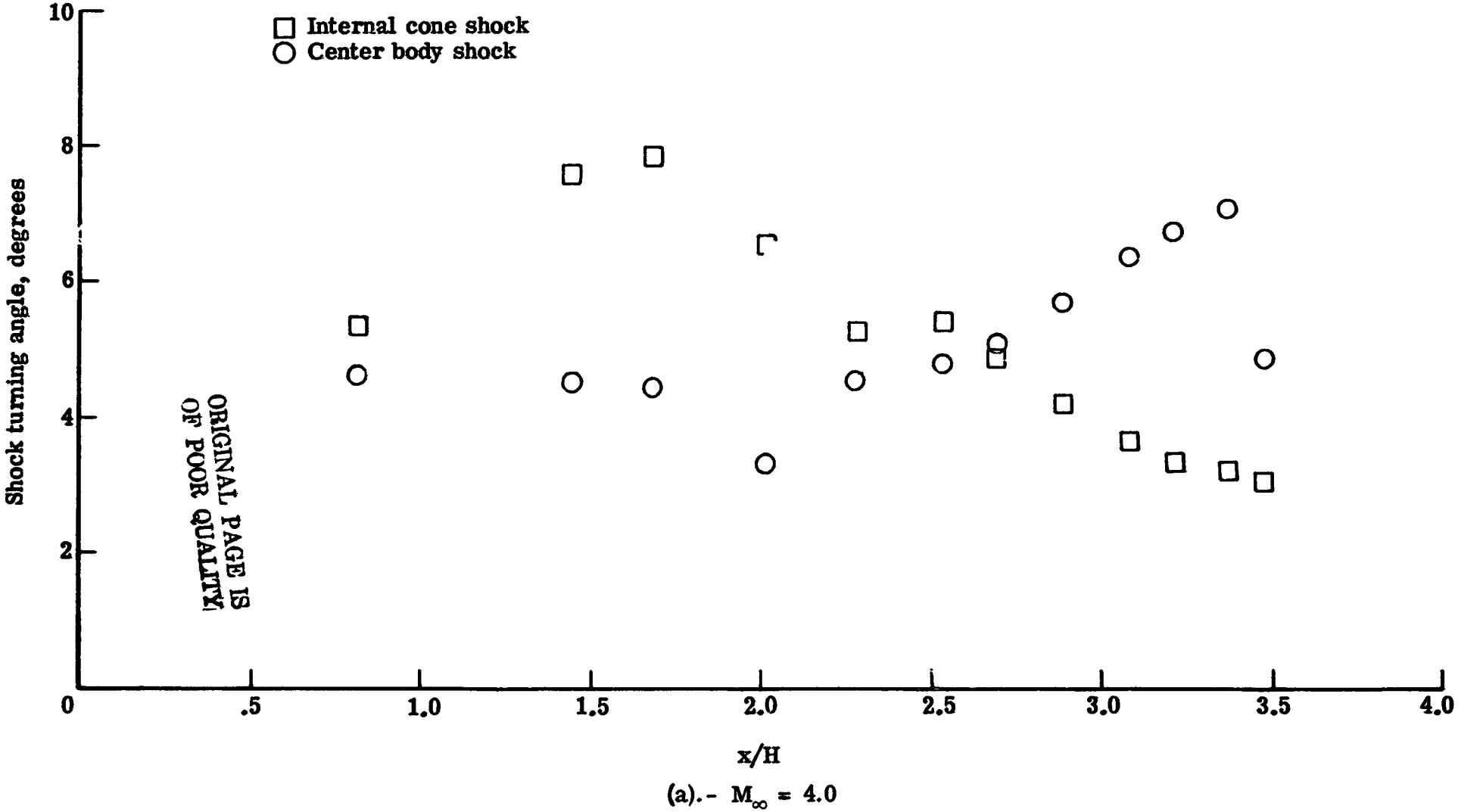

(a).- $M_\infty = 4.0$

Figure 3.- Turning angle through conical shocks for center body cone half angle of 10^o and outer body internal cone angle of 5^o.

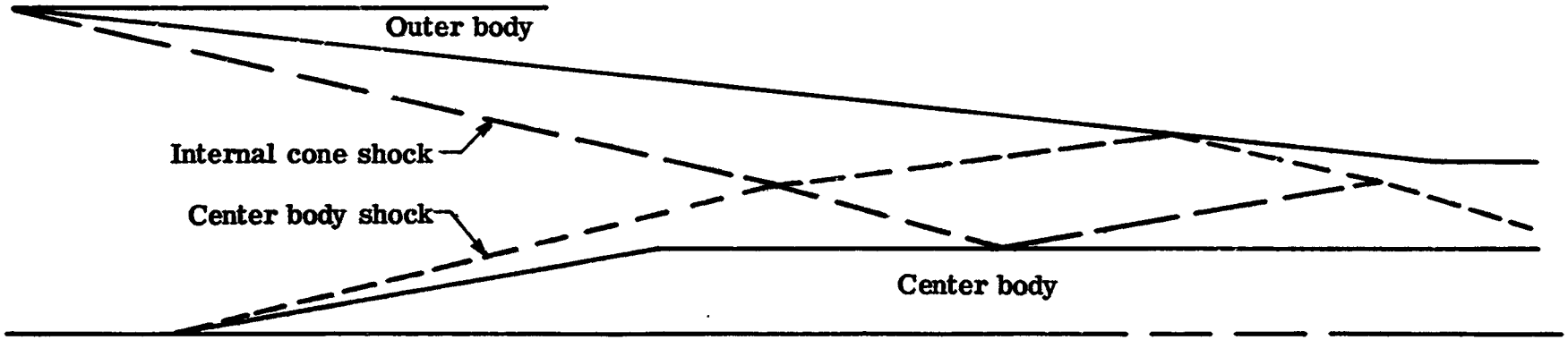

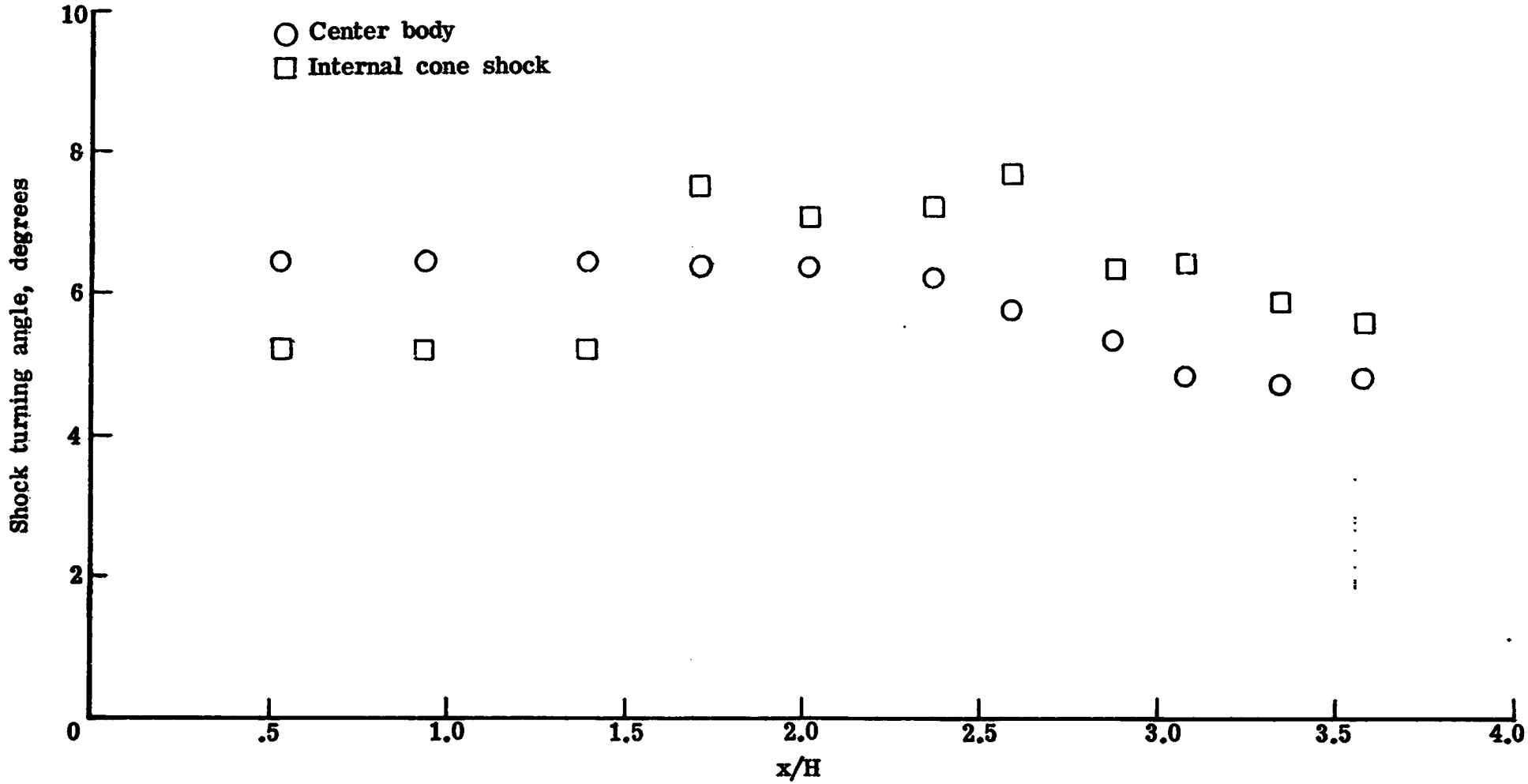

(b).- $M_\infty = 6.0$

Figure 3.- Concluded.

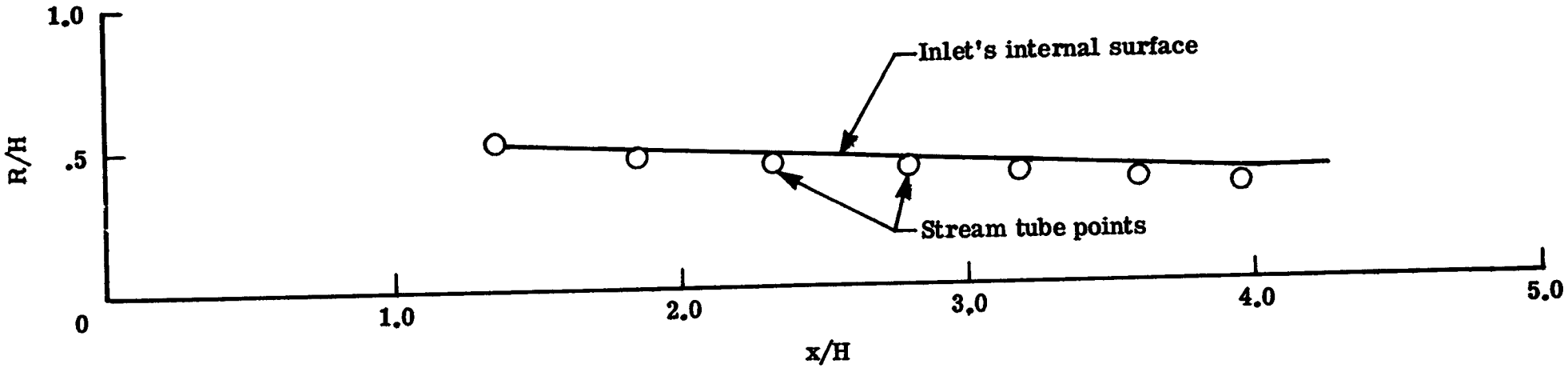

(a).- $\beta = 0^{o}$, $\frac{m}{m_t} = .394$

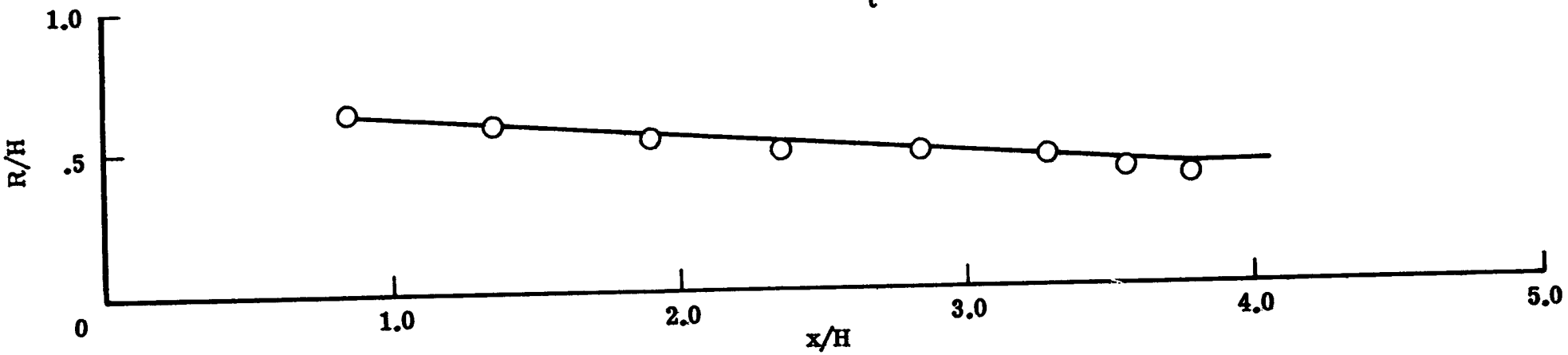

(b).- $\beta = 35.84^{o}$, $\frac{m}{m_t} = .6$

Figure 4.- Axial cross sections of inlet's internal surface as compared with points generated (for $M_1 = 6.0$) from the conical flow field by the stream tube method.

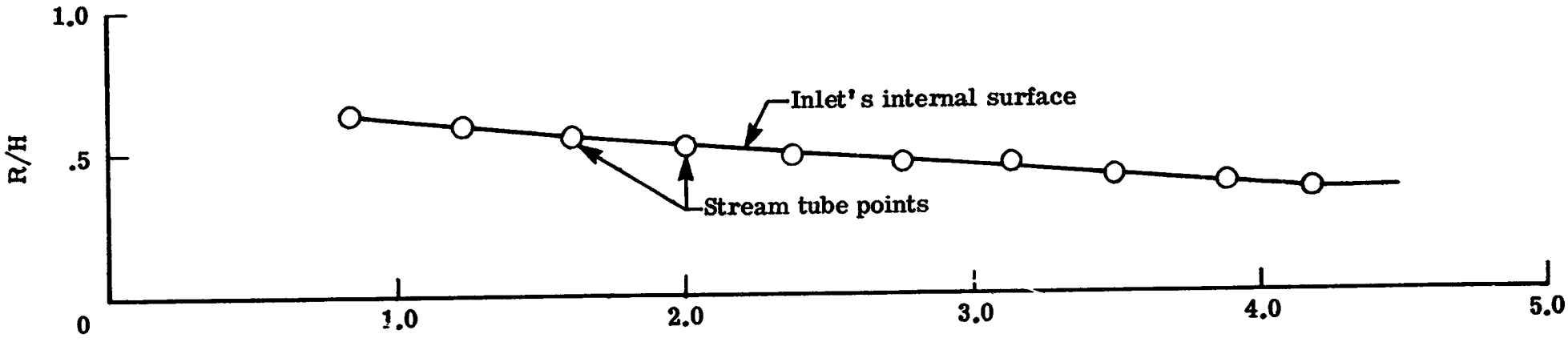

(c).- $\beta = -35.84^{o}$, $\frac{m}{m_t} = .6$

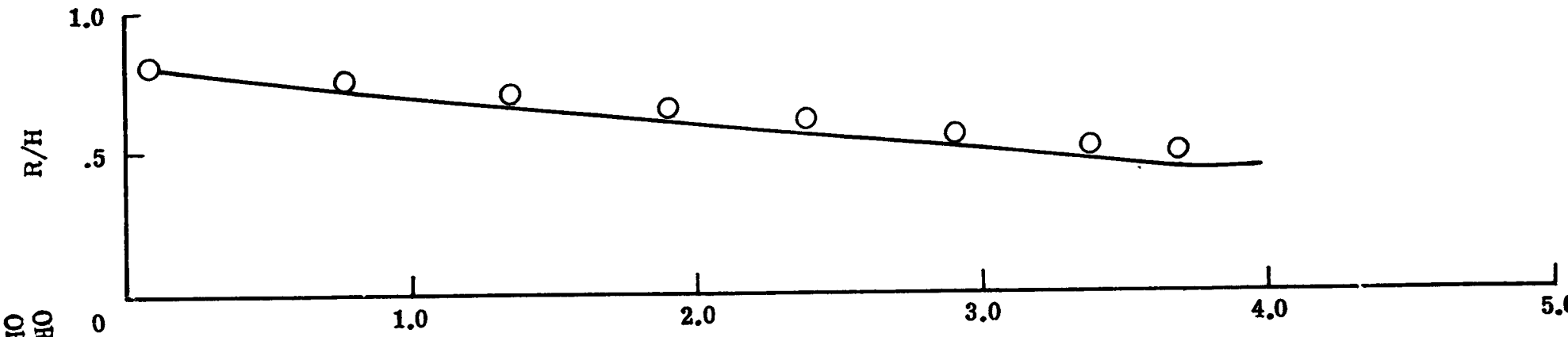

(d).- $\beta = -35.84^{o}$, $\frac{m}{m_t} = 1.0$

Figure 4.- Continued.

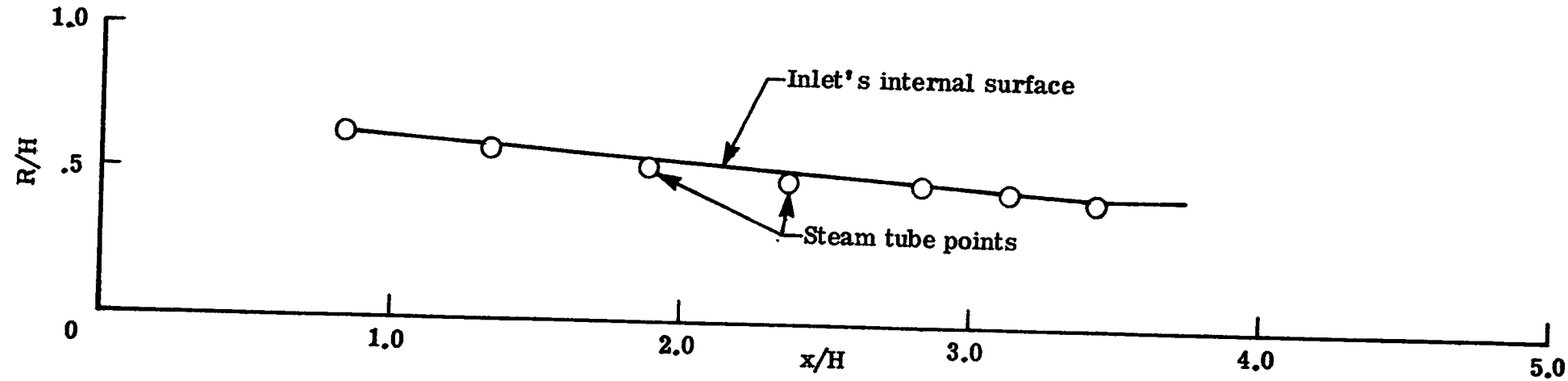

(e).- $\beta = 90^{o}$, $\frac{m}{m_t} = .606$

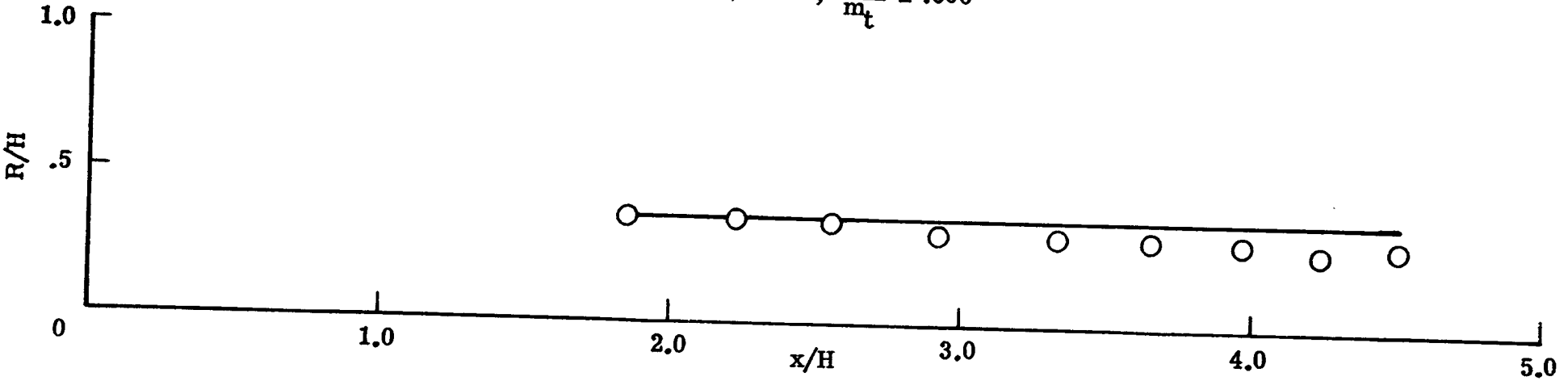

(f).- $\beta = -90^{o}$, $\frac{m}{m_t} = .206$

Figure 4.- Concluded.

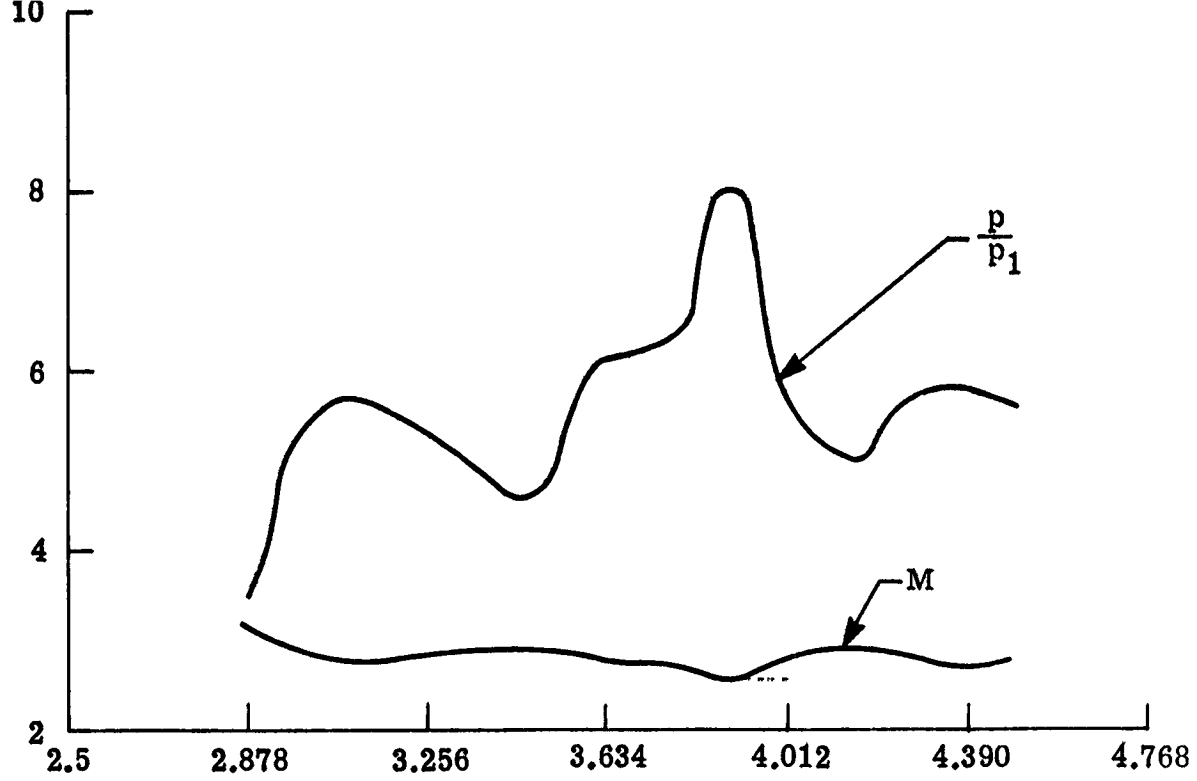

(a).- $M_1 = 4.0$

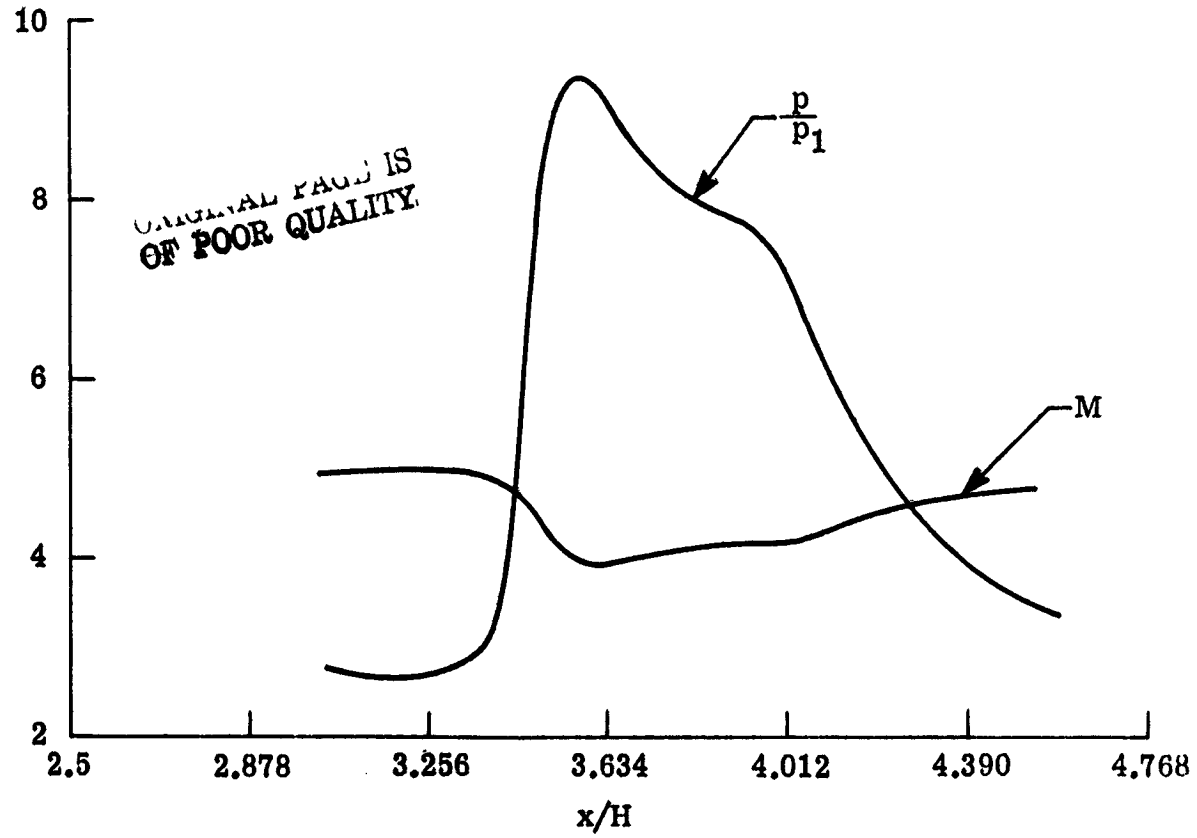

(b).- $M_1 = 6.0$

Figure 5.- Longitudinal distribution of Mach number andppressure ratio on the inlet's internal surface corresponding to $\beta = -90^{o}$.

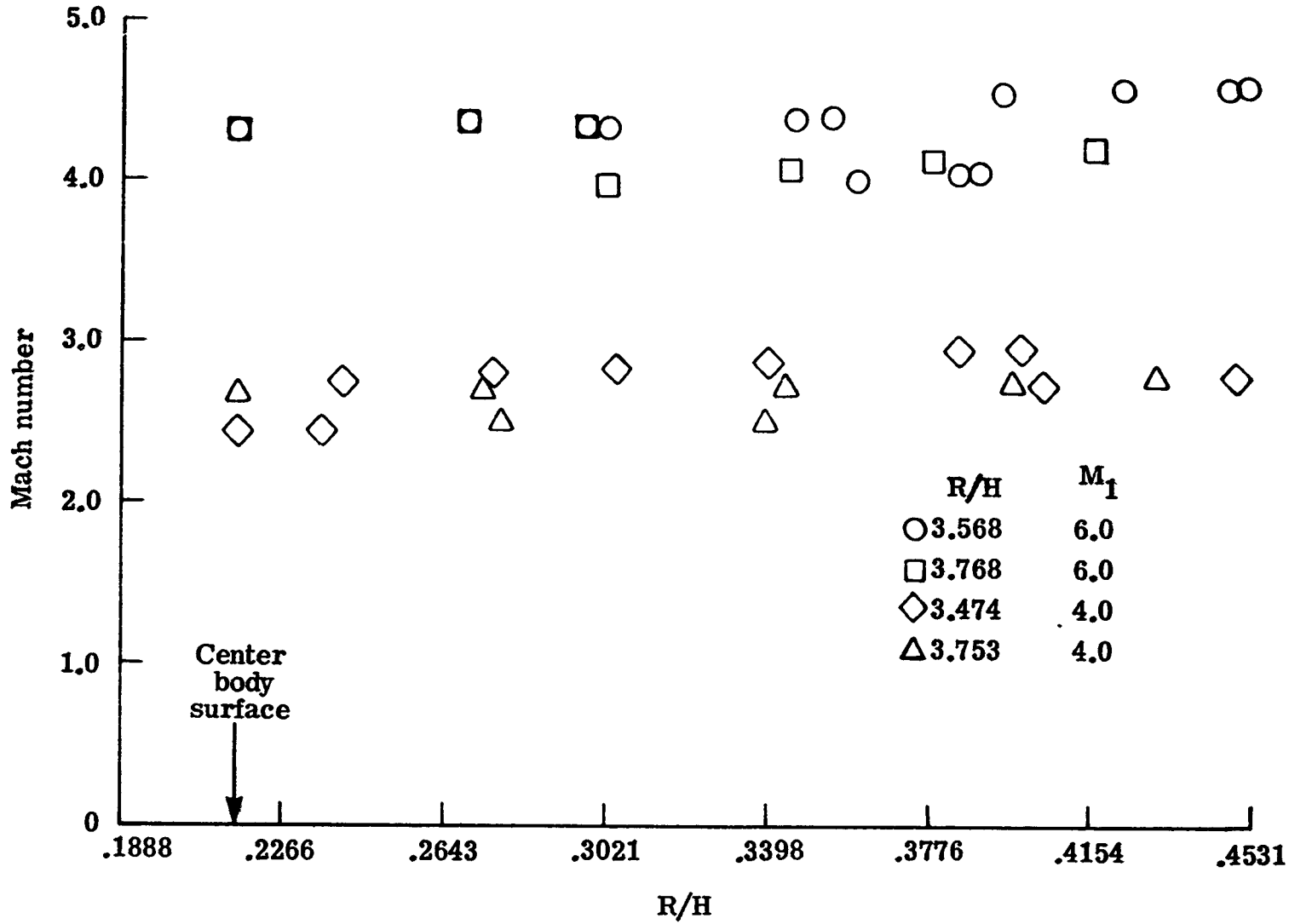

Figure 6.- Mach number distribution in the region of the strut leading edges as determined by conical flow computations.

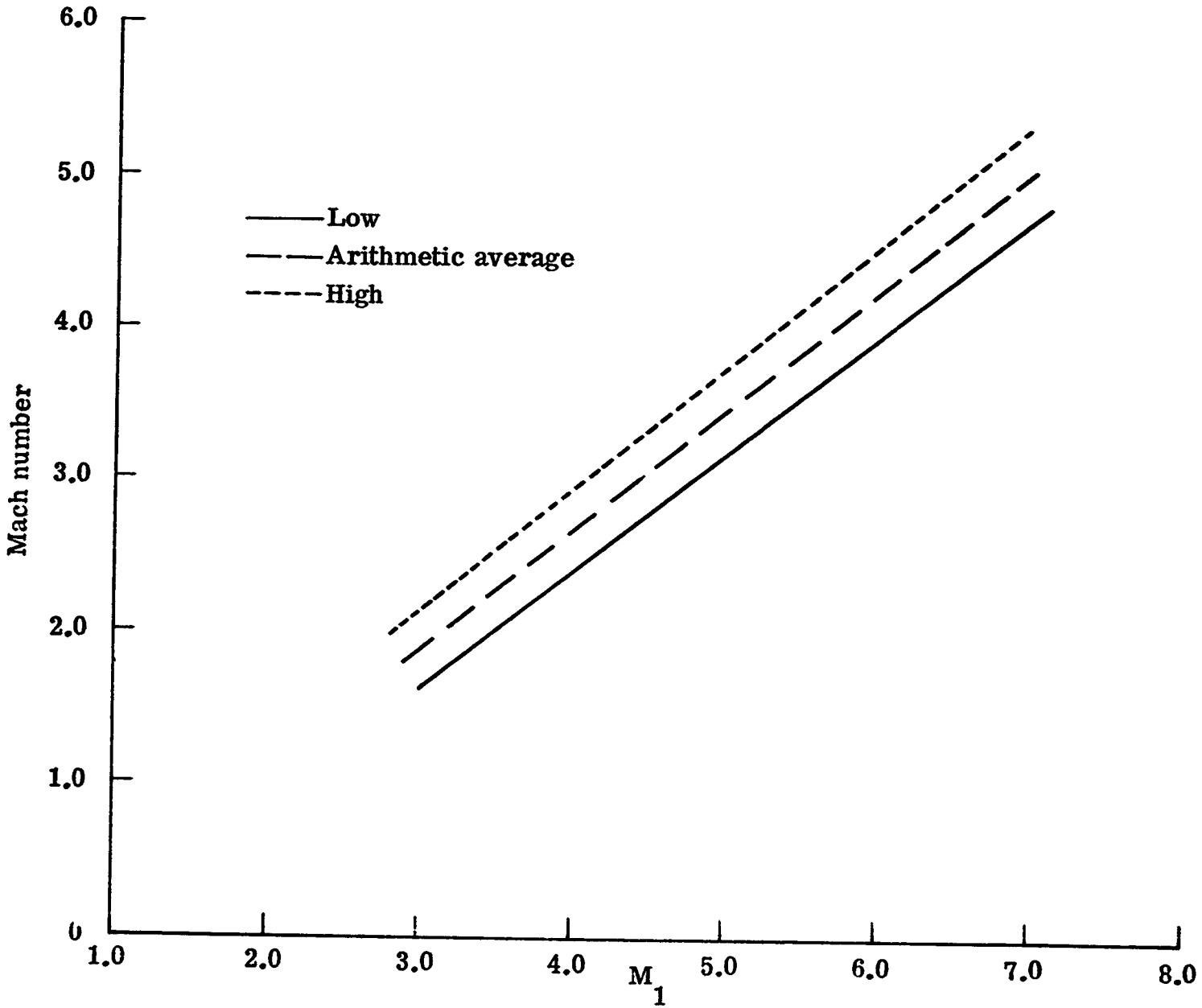

Figure 7.- High, low and arithmetic average values of Mach number in the region of the strut leading edges.

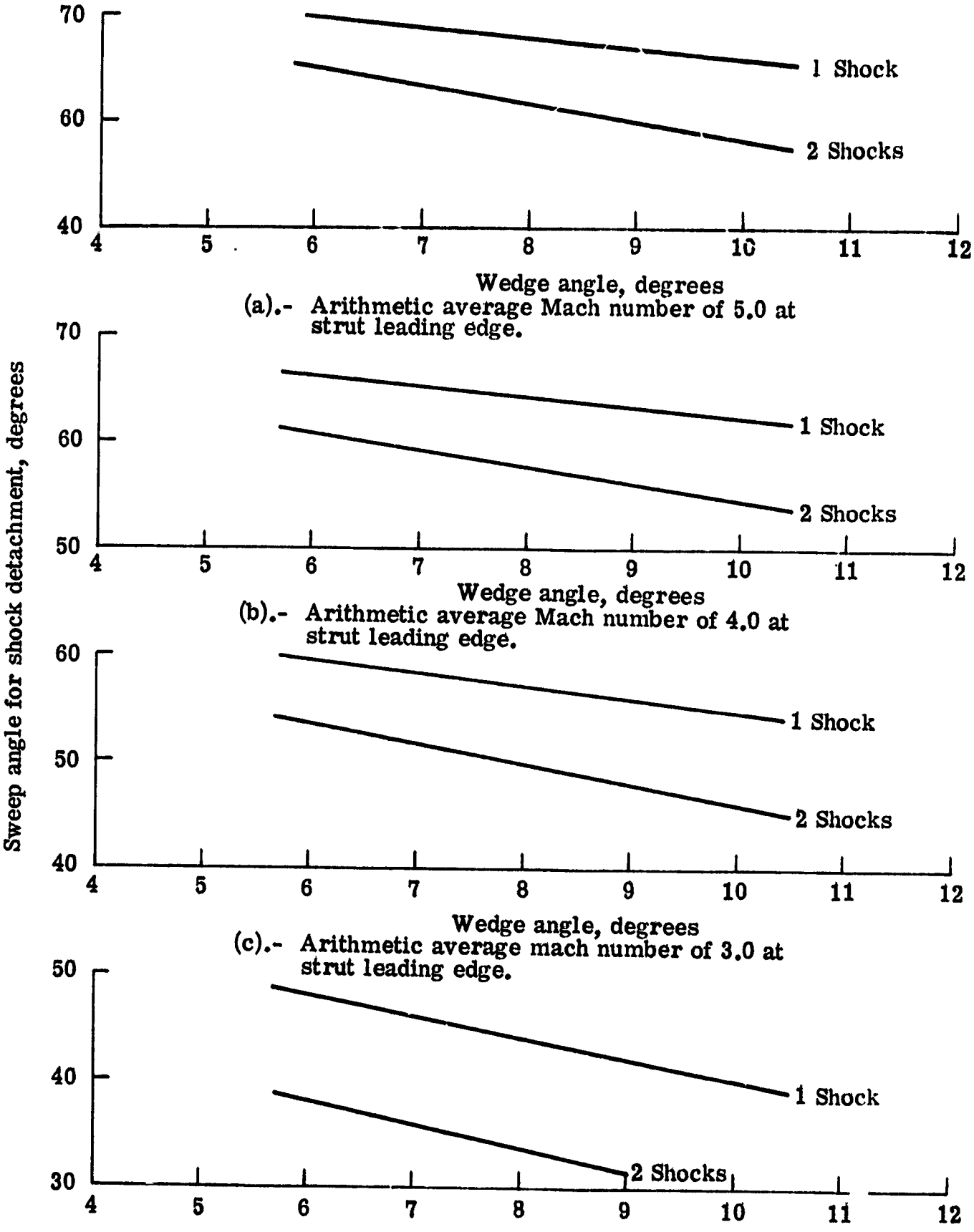

(a).- Arithmetic average Mach number of 5.0 at strut leading edge.

(b).- Arithmetic average Mach number of 4.0 at strut leading edge.

(c).- Arithmetic average mach number of 3.0 at strut leading edge.

Figure 8.-(d).- Arithmetic average Mach number of 2.0 at strut leading edge.

Sweep angle for swept shock detachment in terms of number of shocks.

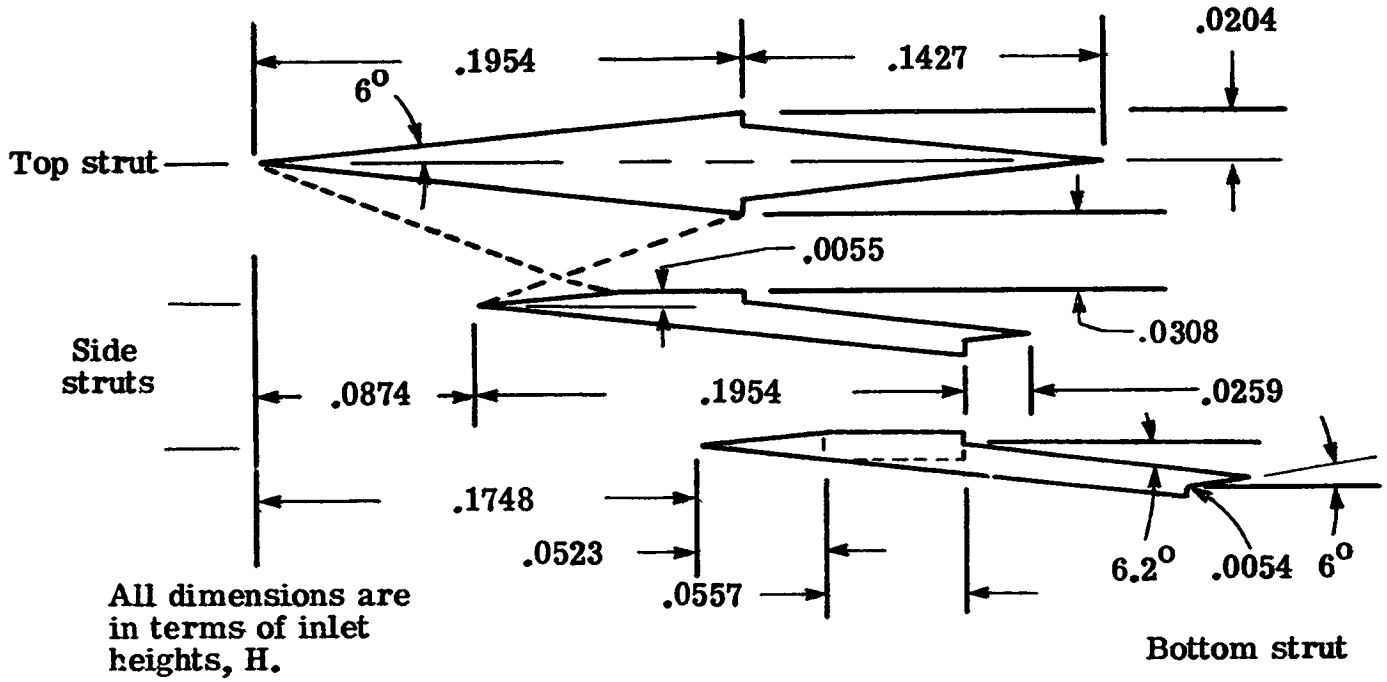

(a).- Typical strut cross sectional design at strut center body surface intersection.

Figure 9 - Strut design and strut configuration.

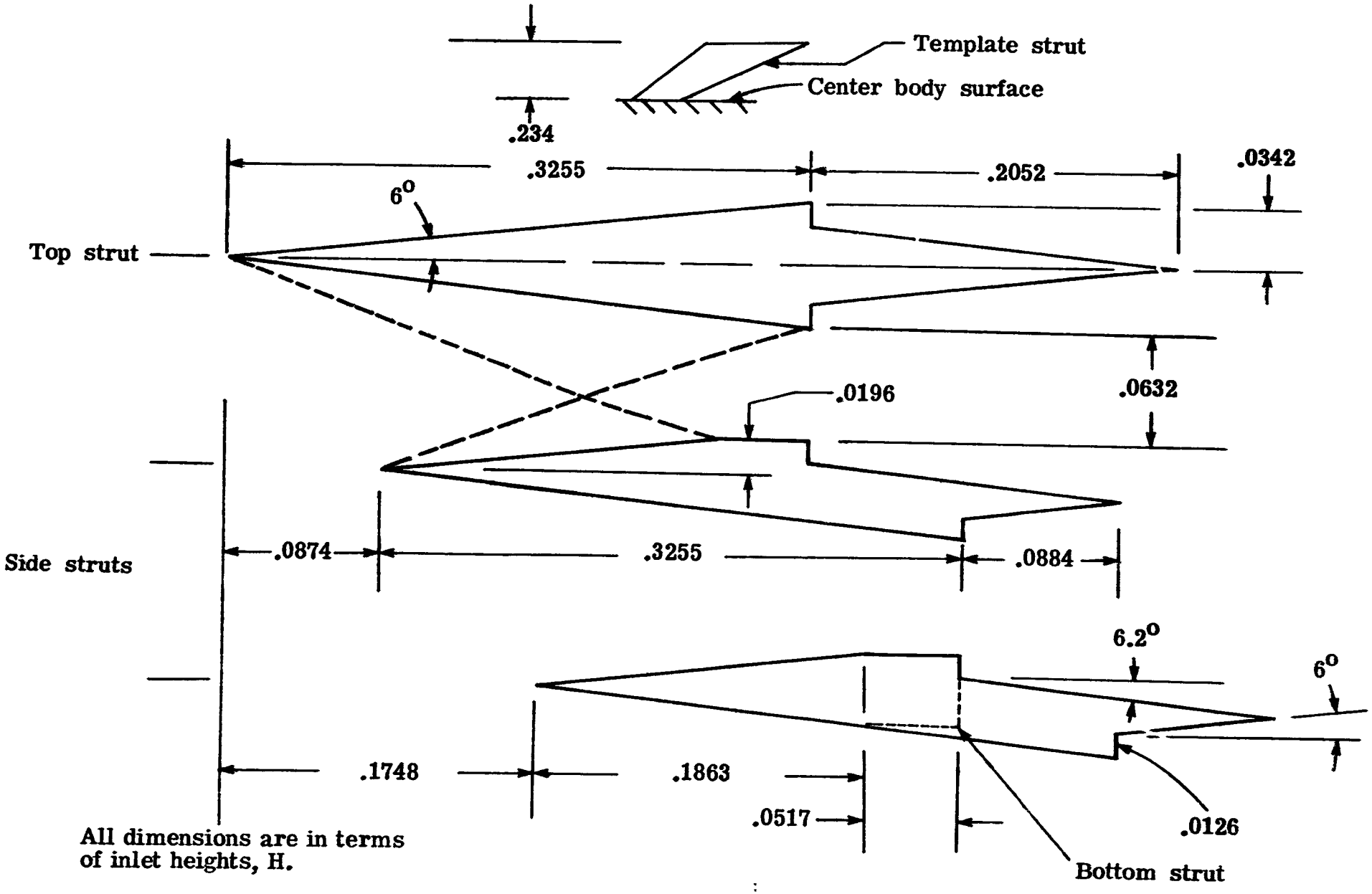

Figure 9.-(b).- Typical strut cross sectional design at outer perimeter corresponding to a strut length of .234 (non-dimensionalized by H). Shorter struts are obtained by cutting off these template struts to appropriate lengths (end away from center body).

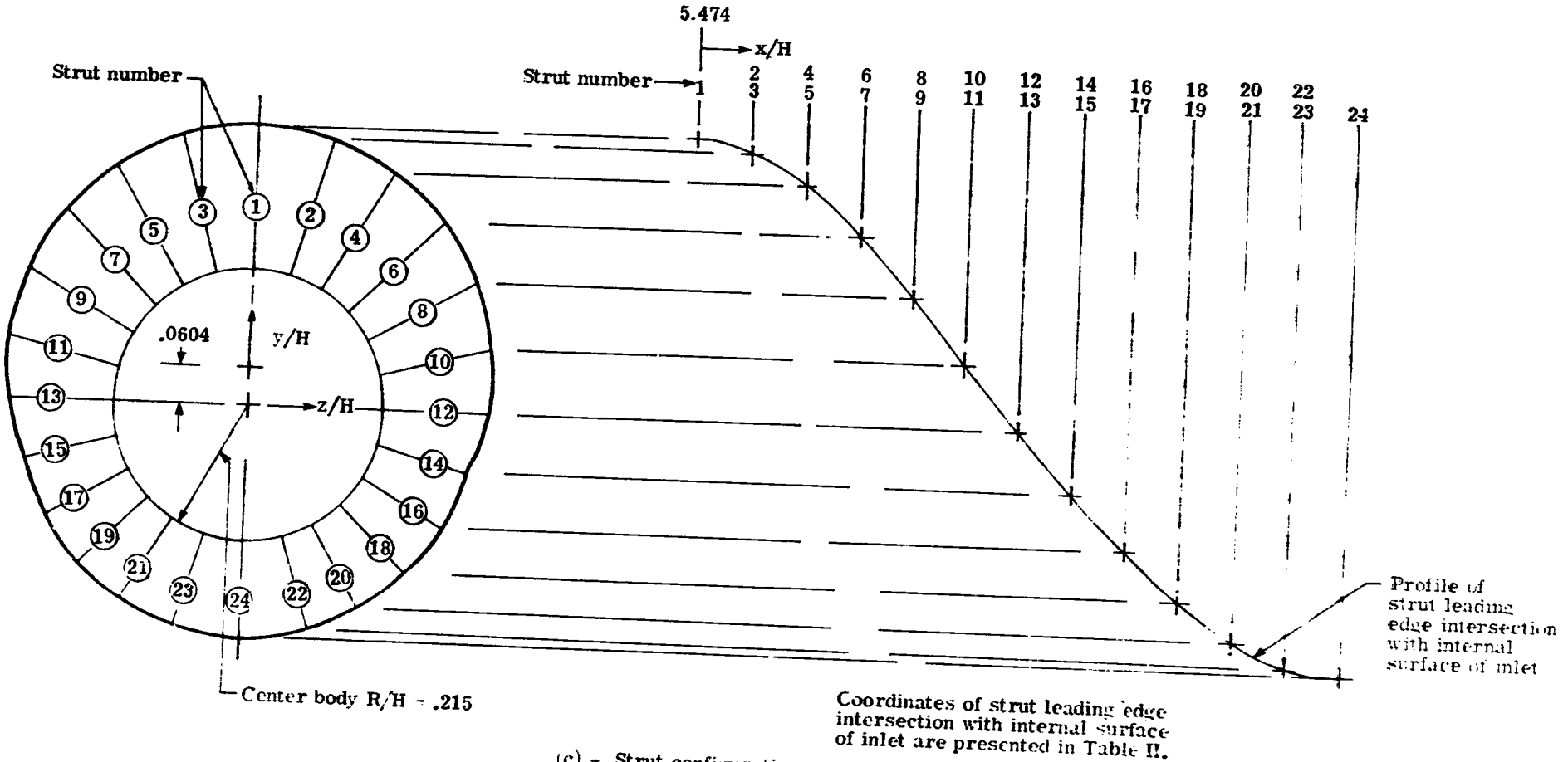

(c).- Strut configuration.

Figure 9 – Concluded

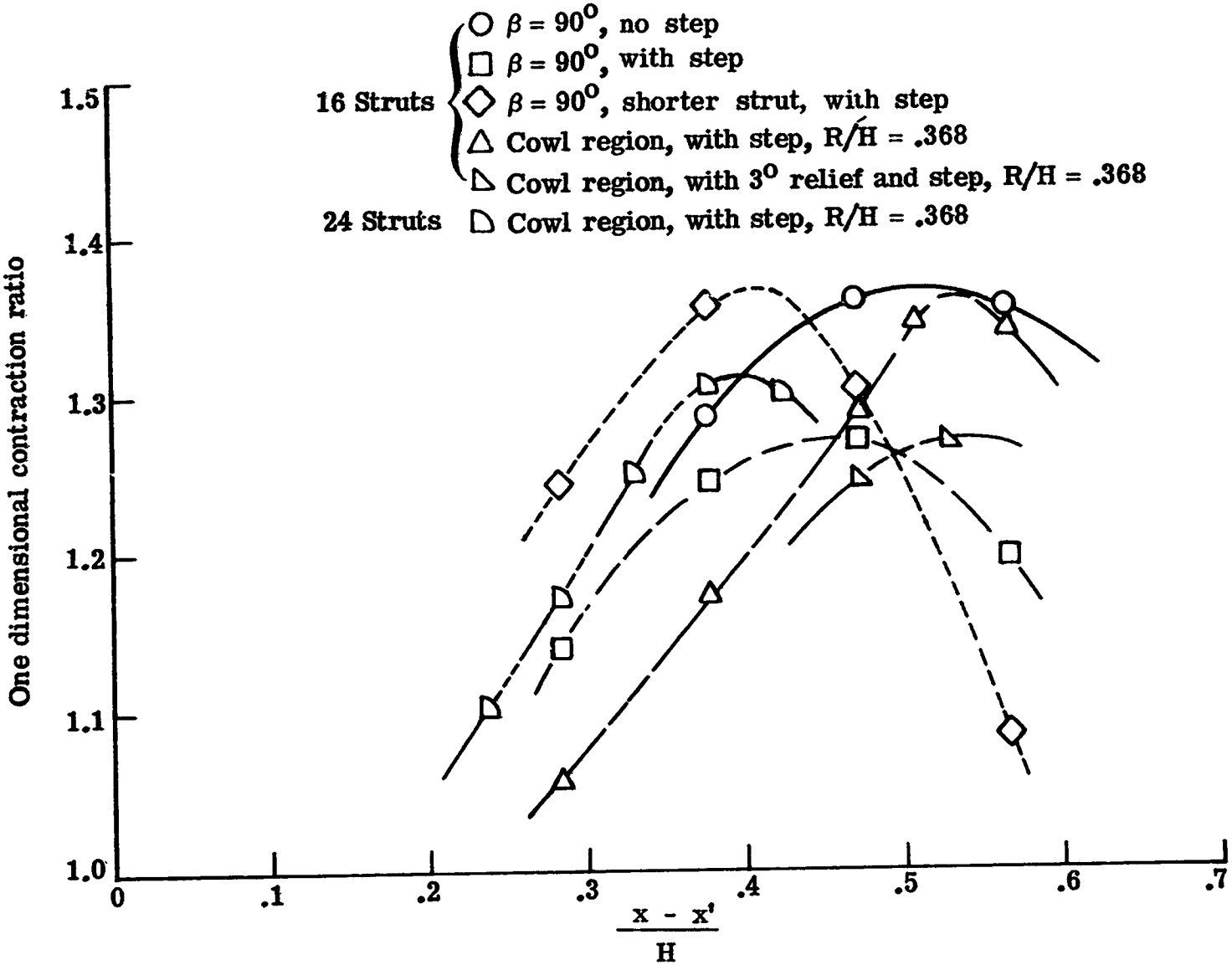

Figure 10.- Area contraction between struts.

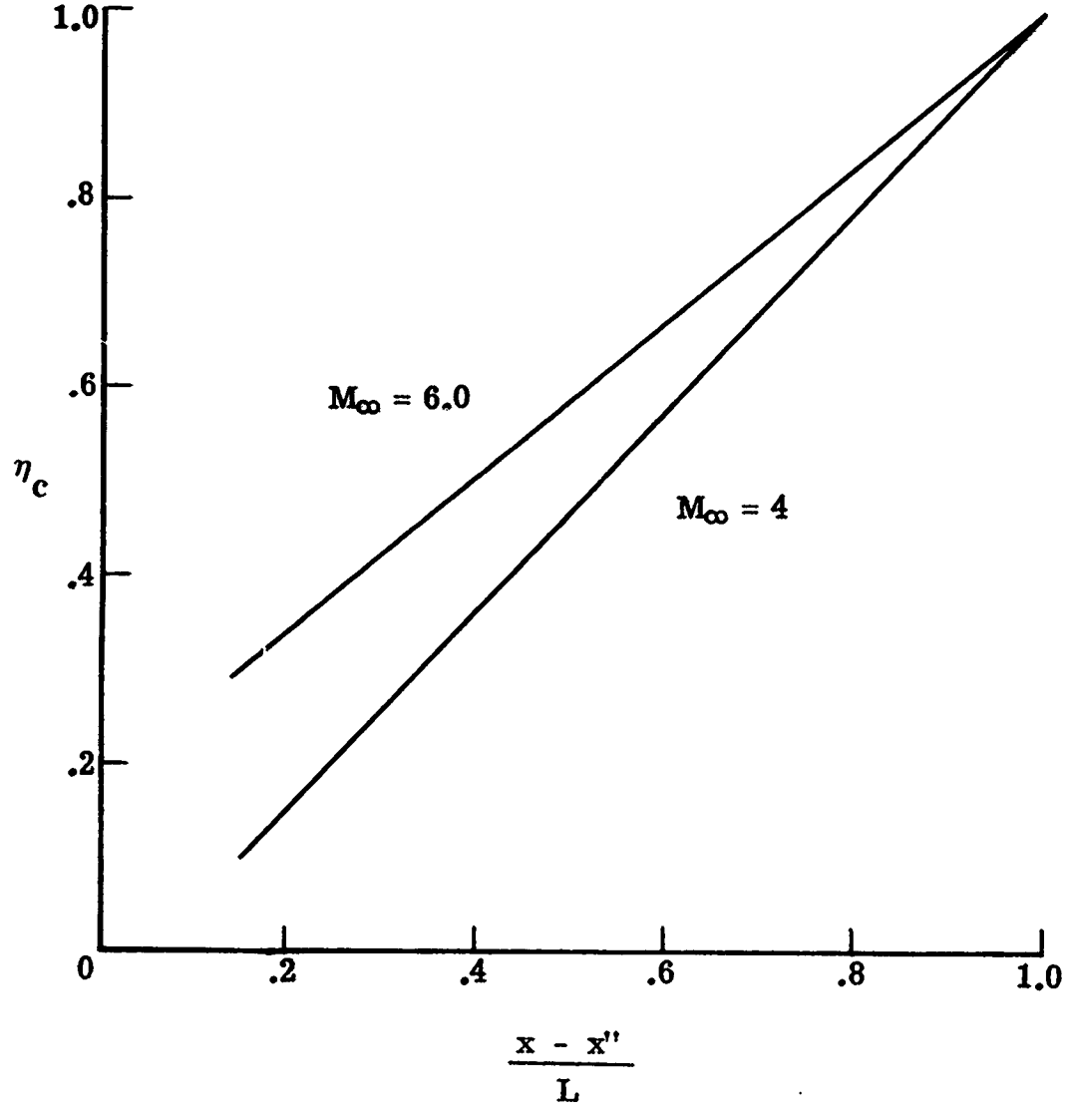

Figure 11.- Combustion efficiency as suggested from cold flow mixing data.

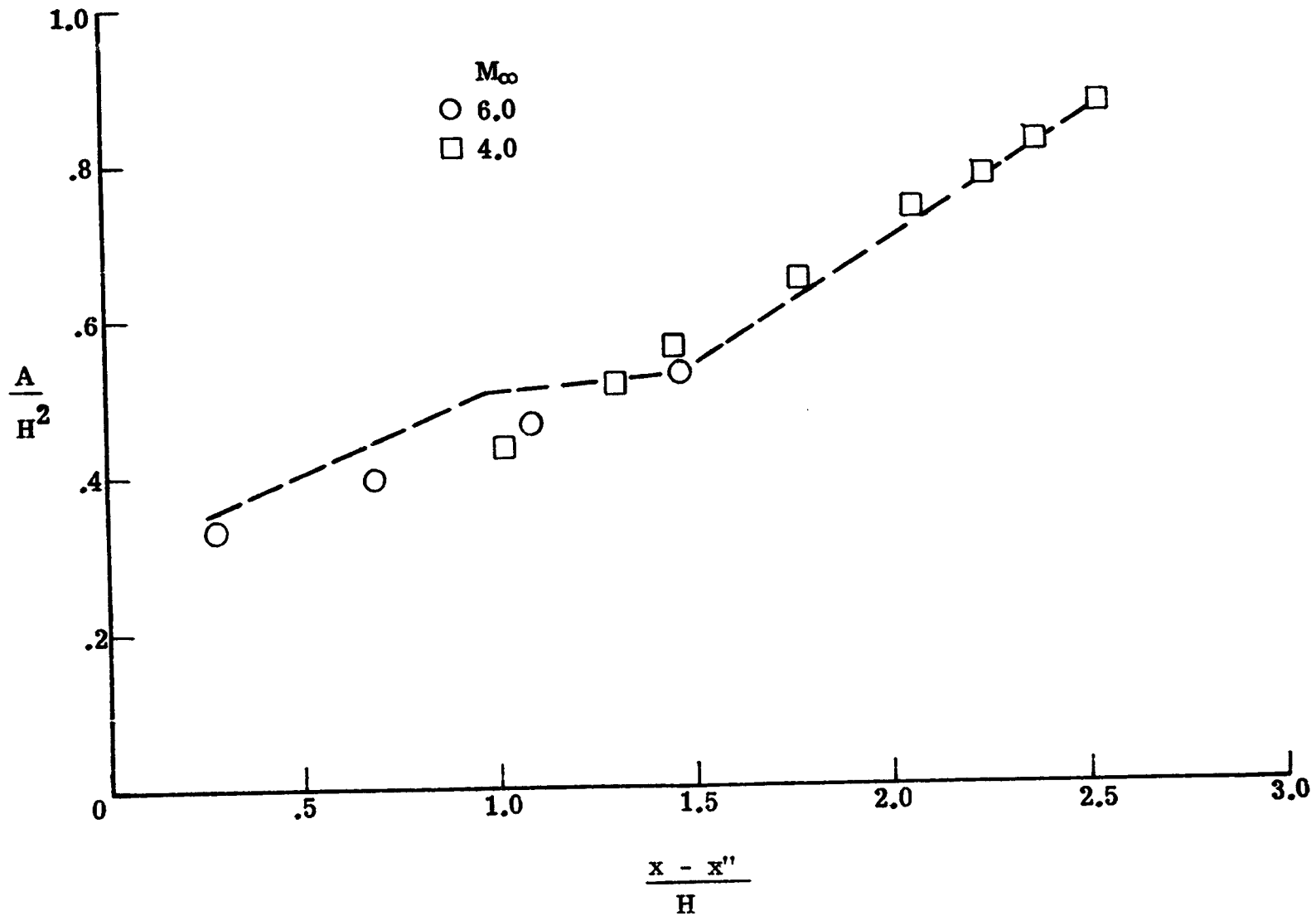

Figure 12.- Combustor area distribution.

1 Report No.	2. Government Accession No.	3. Recipient's Catalog No.
TM-78657		

4. Title and Subtitle	5 Report Date
RECTANGULAR CAPTURE AREA TO CIRCULAR COMBUSTOR SCRAMJET ENGINE	February 1978
	6. Performing Organization Code 3740

7 Author(s)	8 Performing Organization Report No
S. Zane Pinckney	
	10 Work Unit No.
9 Performing Organization Name and Address NASA Langley Research Center Hampton, VA 23665	11. Contract or Grant No
	13 Type of Report and Period Covered Technical Memorandum
12 Sponsoring Agency Name and Address National Aeronautics and Space Administration Washington, D.C. 20546	14 Sponsoring Agency Code

15 Supplementary Notes
This is the final release of special information not suitable for formal publication which serves the following need: To present a new inlet design concept which is to be experimentally tested and evaluated in the future.

16 Abstract

A new concept for a scramjet engine design is presented. The inlet transforms a rectangular shaped capture stream tube into a cross section which is almost circular in shape at the inlet throat or combustor entrance. The inlet inner surface is designed by the method of streamline tracing. The high pressure and temperature regions of the combustor are almost circular in shape and thus the benefits of hoop stresses in relation to structural weight can be utilized to reduce combustor and engine weights. The engine has a center body consisting of a 20^{0} included angle cone, followed by a constant diameter cylinder. Fuel injection struts are arranged in a radial array and are swept 54^{0} from the center body to the inlet inner surface and have values of length to maximum average thickness between 5.6 and 6.6 which are felt to be structurally reasonable. Combustor wetted areas are shown to be less than those of the present fully rectangular engine concept.

17 Key Words (Suggested by Author(s))	18 Distribution Statement
Hypersonic Inlet Inlet Scramjet Hypersonic Propulsion	Unclassified - Unlimited

19 Security Classif (of this report)	20 Security Classif (of this page)	21 No of Pages	22 Price*
Unclassified	Unclassified	44	$4.00

* For sale by the National Technical Information Service Springfield Virginia 22161